A Structural Basis for Metal Ion Mutagenicity and Nucleotide Selectivity in Human DNA Polymerase β[†,‡]

Huguette Pelletier,*[,§] Michael R. Sawaya,[||] William Wolfle,[⊥] Samuel H. Wilson,[⊥] and Joseph Kraut[||]

Department of Chemistry and Biochemistry, University of California, San Diego, La Jolla, California 92093-0506, Sealy Center for Molecular Science, University of Texas Medical Branch, Galveston, Texas 77555-1051, and Verna and Marrs McLean Department of Biochemistry, Baylor College of Medicine, One Baylor Plaza, Houston, Texas 77030

Received December 14, 1995; Revised Manuscript Received June 18, 1996[⊗]

ABSTRACT: When crystals of human DNA polymerase β (pol β) complexed with DNA [Pelletier, H., Sawaya, M. R., Wolfle, W., Wilson, S. H., & Kraut, J. (1996) *Biochemistry 35*, 12742−12761] are soaked in the presence of dATP and Mn^{2+}, X-ray structural analysis shows that nucleotidyl transfer to the primer 3′-OH takes place directly in the crystals, even though the DNA is blunt-ended at the active site. Under similar crystal-soaking conditions, there is no evidence for a reaction when Mn^{2+} is replaced by Mg^{2+}, which is thought to be the divalent metal ion utilized by most polymerases in vivo. These results suggest that one way Mn^{2+} may manifest its mutagenic effect on polymerases is by promoting greater reactivity than Mg^{2+} at the catalytic site, thereby allowing the nucleotidyl transfer reaction to take place with little or no regard to instructions from a template. Non-template-directed nucleotidyl transfer is also observed when pol β−DNA cocrystals are soaked in the presence of dATP and Zn^{2+}, but the reaction products differ in that the sugar moiety of the incorporated nucleotide appears distorted or otherwise cleaved, in agreement with reports that Zn^{2+} may act as a polymerase inhibitor rather than as a mutagen [Sirover, M. A., & Loeb, L. A. (1976) *Science 194*, 1434−1436]. Although no reaction is observed when crystals are soaked in the presence of dATP and other metal ions such as Ca^{2+}, Co^{2+}, Cr^{3+}, or Ni^{2+}, X-ray structural analyses show that these metal ions coordinate the triphosphate moiety of the nucleotide in a manner that differs from that observed with Mg^{2+}. In addition, all metal ions tested, with the exception of Mg^{2+}, promote a change in the side-chain position of aspartic acid 192, which is one of three highly conserved active-site carboxylate residues. Soaking experiments with nucleotides other than dATP (namely, dCTP, dGTP, dTTP, ATP, ddATP, ddCTP, AZT-TP, and dATPαS) reveal a non-base-specific binding site on pol β for the triphosphate and sugar moieties of a nucleotide, suggesting a possible mechanism for nucleotide selectivity whereby triphosphate−sugar binding precedes a check for correct base pairing with the template.

The requirement of divalent metal ions for catalysis was recognized early in the study of *Escherichia coli* DNA polymerase I (Bessman et al., 1958), and subsequent studies with other polymerases have since confirmed that Mg^{2+} is probably the divalent metal ion utilized by most polymerases for catalysis in vivo (Kornberg & Baker, 1992). On the basis of structures of ternary complexes of rat DNA polymerase β (pol β) with template-primer and ddCTP substrates, specific roles have been assigned for two Mg^{2+} ions in the active site of pol β (Figure 1) (Pelletier et al., 1994). Such a detailed view of the active site offered an explanation for how a potent metal ion mutagen such as Mn^{2+} (Demerec & Hanson, 1951; Berg et al., 1963; Orgel & Orgel, 1965; Hall & Lehman, 1968; van de Sande et al., 1972; Chang & Bollum, 1973; Dube & Loeb, 1975; Linn et al., 1976; Stoner et al., 1976; Gillin & Nossal, 1976; Sirover & Loeb, 1976a, 1977; Wang et al., 1977; Seal et al., 1978; Sirover et al., 1979; Kunkel & Loeb, 1979; Hibner & Alberts, 1980; Krauss & Linn, 1980; Fersht et al., 1983; Goodman et al., 1983; El-Deiry et al., 1984, 1988; Beckman et al., 1985; Tabor & Richardson, 1989; Copeland et al., 1993) might cause a polymerase to make errors during DNA replication: a change from Mg^{2+} to Mn^{2+} as the nucleotide-binding metal ion, for instance, could result in just enough mispositioning of the nucleotide[1] in the active site to make it difficult for the polymerase to distinguish among a ribonucleoside triphosphate (NTP),[2] a deoxynucleoside triphosphate (dNTP), and a dideoxynucleoside triphosphate (ddNTP) (Figure 1).

With at least three different types of metal ion binding sites now recognized for a polymerase such as pol β—one catalytic (Pelletier et al., 1994), one nucleotide-binding (Pelletier et al., 1994), and two additional DNA-binding (Pelletier et al., 1996; Pelletier & Sawaya, 1996)—it is

[†] Supported by NIH Grants GM52860 and ES06839 and by R. A. Welch Foundation Grant H-1265.

[‡] Coordinates and reflection data are available from the Brookhaven Protein Data Bank and may also be obtained by sending an e-mail request to hug@bcm.tmc.edu.

* To whom correspondence should be addressed.

[§] Baylor College of Medicine.

[||] University of California, San Diego.

[⊥] Sealy Center for Molecular Science.

[⊗] Abstract published in *Advance ACS Abstracts,* September 1, 1996.

[1] The word nucleotide is meant to be a general term referring to any compound that possesses a base, a sugar, and a phosphate moiety. Also, depending on the context, a nucleotide can either be covalently linked as a part of a DNA strand, as in the terminal nucleotide (or the terminal dNMP) of the primer strand, or a nucleotide can be a free-standing entity, as in the incoming nucleotide (or the incoming dNTP) for the reaction at the active site. Similarly, the word sugar is meant to be a general term and could represent a ribose, a deoxyribose, a dideoxyribose, or even a 3′-azido-2′,3′-dideoxyribose (as is the case when discussing the sugar moiety of AZT-TP).

S0006-2960(95)02956-4 CCC: $12.00

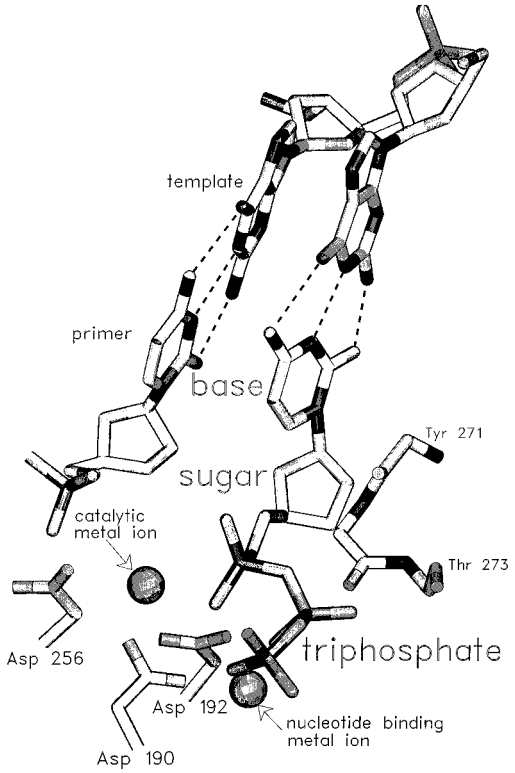

FIGURE 1: SETOR diagram (Evans, 1993) showing the active site of the rat pol β−DNA−ddCTP ternary complex structure crystallized in space group $P6_1$ (Pelletier et al., 1994). For clarity, the only parts of pol β depicted are the active-site carboxylate residues (aspartic acids 190, 192, and 256) and the peptide backbone of the sugar-selective protein segment (tyrosine 271−threonine 273) of the thumb subdomain. The base, sugar, and triphosphate moieties of the nucleotide are labeled to highlight the various tiers of selectivity that an incoming nucleotide may encounter at the active site. The catalytic metal ion is proposed to stabilize the pentacoordinated α-phosphate of the transition state, while the nucleotide-binding metal ion, which coordinates the triphosphate moiety of the nucleotide, is proposed to help position the nucleotide for catalysis, although both metal ions probably carry out both functions to some extent (Pelletier et al., 1994). The catalytic metal ion has been observed in pol β crystal structures in both the presence and absence of DNA or nucleotide substrates, but the nucleotide-binding metal ion has never been observed in our pol β crystal structures except when accompanied by a nucleotide or pyrophosphate and should, in effect, be considered as a part of the nucleotide (Pelletier et al., 1994; Sawaya et al., 1994; Pelletier, 1994; Pelletier & Sawaya, 1996). The recent discovery that pol β belongs to an ancient nucleotidyltransferase superfamily (Holm & Sander, 1996) suggests that the nucleotidyl transfer mechanism for pol β may be applicable to many non-DNA-polymerizing nucleotidyltransferases, like kanamycin nucleotidyltransferase (Pedersen et al., 1995), as well.

evident that sorting out the individual influences that a given metal ion mutagen has on the processivity and overall fidelity of any polymerase can be complicated. A good example of this is provided by the metal ion Ni^{2+}, where vastly different effects on processivity and fidelity have been observed with various polymerases (Snow et al., 1993). Our crystallographic study of the metal ion binding behavior of human pol β extends beyond Mg^{2+} and Ni^{2+} to include seven other metal ions as well (Ca^{2+}, Cd^{2+}, Co^{2+}, Cr^{3+}, Cu^{2+}, Mn^{2+}, and Zn^{2+}), some of which have been classified as general polymerase mutagens and potential carcinogens (Sirover & Loeb, 1976a). Before a structural basis for metal ion mutagenicity in pol β is discussed, however, it is perhaps best, for the sake of clarity, to separate the types of errors that a polymerase can make into two categories: (i) errors caused by slippage between the the template and the primer strands during DNA replication and (ii) errors caused by a breakdown in nucleotide selectivity in the active site.

DNA misalignment errors, where mistakes in DNA replication are the result of slippage between the template and the primer (error type i above) (Streisinger et al., 1966; Kunkel, 1992), have received attention lately because of recent observations that the DNA in cancer cells show an inordinate frequency of misalignment errors when compared with the DNA of normal cells[3] (Strand et al., 1993; Kunkel, 1993). In vitro studies have linked polymerase misalignment errors with pause sites (Fry & Loeb, 1992; Bebenek et al., 1993) (that is, special sequences in the DNA template, typically nucleotide repeats, that cause a polymerase to slow down or completely dissociate from the template during processive polymerization), and a working hypothesis for DNA and RNA polymerases is that a slower rate of dissociation from a template-primer substrate is usually accompanied by a lower incidence of misalignment errors. This has been amply demonstrated by studies with *E. coli* DNA polymerase I (Eckert & Kunkel, 1993a) as well as with human DNA polymerase α and HIV-1 reverse transcriptase (Eckert & Kunkel, 1993b); in all three cases, a decrease in the pH of the polymerase reaction medium resulted in an increase in processivity (slower rate of dissociation from the DNA), which in turn was accompanied by a decrease in misalignment errors. There is some evidence that, in addition to pH, certain metal ions can have a direct effect on processivity and misalignment errors as well (Snow & Xu, 1991; Snow et al., 1993). Pol β, in particular, has been shown to be markedly more processive on template-primer substrates when Mg^{2+} is replaced by Mn^{2+} in the reaction medium (Wang & Korn, 1982), and this increase is processivity is accompanied by a decrease in misalignment errors (Kunkel, 1985).

Crystal soaking experiments have been performed in an attempt to characterize more fully the metal ion binding helix−hairpin−helix (HhH) motifs in the 31-kDa and the 8-kDa domains of pol β and to determine which, if any, of the aforementioned metal ions may bind to the HhH sites and possibly alter DNA binding (Pelletier & Sawaya, 1996). Although there is evidence that each of the aforementioned metal ions is capable of binding to HhH metal sites, it was also shown that the HhH motifs are highly selective for K^+ and Na^+ and that transition metal ions do not compete well with these biologically prevalent metal ions for binding in the HhH metal sites (Pelletier & Sawaya, 1996). These results suggest that potential metal ion mutagens may alter

[2] Abbreviations; ATP, adenosine 5′-triphosphate; AZT-TP, 3′-azido-2′,3′-dideoxythymidine triphosphate; dATP, 2′-deoxyadenosine 5′-triphosphate; dATPαS, 2′-deoxyadenosine 5′-*O*-(1-thiotriphosphate); dCTP, 2′-deoxycytidine 5′-triphosphate; ddATP, 2′,3′-dideoxyadenosine 5′-triphosphate; ddCTP, 2′,3′-dideoxycytidine 5′-triphosphate; ddNTP, 2′,3′-dideoxynucleoside 5′-triphosphate; dGTP, 2′-deoxyguannosine 5′-triphosphate; dNMP, 2′-deoxynucleoside 5′-monophosphate; dNTP, 2′-deoxynucleoside 5′-triphosphate; dTTP, thymidine 5′-triphosphate; HhH, helix−hairpin−helix; MES, 2-(*N*-morpholino)ethanesulfonic acid; NTP, ribonucleoside triphosphate; PDB, Brookhaven Protein Data Bank; 6bp, structure of pol β complexed with 6 base pairs of DNA; 7bp, structure of pol β complexed with 7 base pairs of DNA.

[3] Typical genomic DNA has many tandemly repeated sequences, or microsatellites, that are 1−6 nucleotides long, and it is thought that in normal cells numerous misalignment errors are made on such templates during replication but are then repaired by postreplicative DNA repair mechanisms, whereas in certain cancer cells the postreplicative DNA repair machinery fails to function properly, resulting in highly mutated, carcinogenic DNA (Strand et al., 1993; Kunkel, 1993).

pol β−DNA interactions and affect processivity (that is, possibly affect the frequency of misalignment errors) in a more subtle fashion than binding directly in the HhH metal sites in vivo.

In contrast to possible metal ion effects on DNA binding, processivity, and misalignment errors, the work presented here focuses solely on nucleotide selectivity in the active site (related to polymerase error type ii above) and the possible ways that a metal ion mutagen can cause a polymerase such as pol β to incorporate an incorrect nucleotide and thereby decrease fidelity. In that a given nucleotide can be subdivided into three distinct segments (the base, the sugar, and the triphosphate moieties), and because it is possible for the triphosphate moiety of a nucleotide to be coordinated by a number of different metal cations, an incoming nucleotide may encounter several tiers of selectivity in the active site of a polymerase (Figure 1). As an example, early studies of nucleotide selectivity have addressed questions concerning only base substitution errors and the role of the DNA template in guiding complementary base-pairing during replication processes (Watson & Crick, 1953; Trautner et al., 1962; Freese & Freese, 1967). However, the advent of dideoxynucleotide inhibitors as anti-HIV drugs (Yarchoan et al., 1989; Schinazi, 1993), as well as the development of new methods for improving polymerase chain reaction (PCR) techniques with various metal ion−dideoxynucleotide combinations (Tabor & Richardson, 1989, 1990, 1995), has created interest in studying polymerase active sites specifically for their ability to distinguish a correct from an incorrect sugar moiety of the nucleotide. In addition, the use of phosphorothioate nucleotide derivatives in polymerase kinetic experiments (Burgers & Eckstein, 1979; Kuchta et al., 1987; Patel et al., 1991; Wong et al., 1991; Spence et al., 1995; Werneburg et al., 1996) has also shifted some of the focus away from the base moiety and raises questions concerning selectivity and binding of the triphosphate moiety of the nucleotide.

In an attempt to expand our understanding of nucleotide selectivity in the active site of pol β, crystal soaking experiments have been performed on previously described human pol β−DNA complex crystals (Pelletier et al., 1996) in the presence of various metal ions and nucleotides, and in each case, an X-ray structural analysis has been carried out. In one set of experiments, the type of nucleotide utilized (dATP) remained constant while the type of metal ion in the soaking solution varied among Ca^{2+}, Cd^{2+}, Co^{2+}, Cr^{3+}, Cu^{2+}, Mg^{2+}, Mn^{2+}, Ni^{2+}, and Zn^{2+}, and in a second set of crystal soaking experiments, the type of metal ion utilized (Mn^{2+}) was held constant while the nucleotide was varied with respect to the base (dATP, dCTP, dGTP, dTTP), the sugar (ATP, ddATP, AZT-TP), or the triphosphate (dATPαS). Although the DNA is blunt-ended at the active site in these crystals (that is, there is no template overhang available for base-pairing with an incoming nucleotide), significant differences could be observed in nucleotide binding in the active site of pol β with relatively little change in the constitution of the soaking solution, and the cumulative results from over 60 different crystal soaking experiments offer a structural basis for metal ion mutagenicity and nucleotide selectivity in pol β that may be applicable to all polymerases.

EXPERIMENTAL PROCEDURES

Crystal Soaks. Crystallization of two slightly different human DNA pol β−DNA binary complexes, designated as 6bp and 7bp, respectively (Figure 2), were carried out as described (Pelletier et al., 1996). In order to standardize the soaking experiments, crystals were gradually introduced to an artificial mother liquor (16% PEG 3350, 150 mM NaCl, and 100 mM MES, pH 6.5) by periodic addition of small amounts of the artificial mother liquor directly into the crystallization drop. When it became apparent that no damage would be done to the crystals by a complete transfer into artificial mother liquor, crystals of comparable size (typically the largest two or three crystals in a given drop) were collected into a single well of an MVD-24 sitting drop tray (Charles Supper Co.) (the 6bp and 7bp crystals were gathered into separate wells), and after a brief rinsing with artificial mother liquor, the crystals were allowed to equilibrate in artificial mother liquor for at least 48 h before any given soaking experiment began. A typical soaking experiment therefore started with a crystal taken from only one of two different wells—either the common well where all the 6bp crystals were gathered and equilibrated or the common well where all the 7bp crystals were gathered and equilibrated.

All nucleotides (ATP, dATP, ddATP, dCTP, ddCTP, dGTP, dTTP, and dATPαS) were purchased from Pharmacia Biotech, with the exception of AZT-TP, which was purchased from Moravek Biochemicals. Soaking solutions were made by starting with 1 mL of artificial mother liquor and then adding micromolar quantities of concentrated stock solutions (in deionized and distilled H_2O) of various metal ions and nucleotides, resulting in the final concentrations listed under soaking conditions (Table 1). For each soaking experiment a single preequilibrated crystal in artificial mother liquor was placed in a well of an MVD-24 sitting drop tray, and after a brief rinse with a designated soaking solution, the crystal was left to soak in about 150−200 μL of the soaking solution. The remaining 700−800 μL of solution was placed in the reservoir to prevent drying out of the drop, and the reservoir and drop were sealed with clear packaging tape (Manco, purchased from Sears). Unless otherwise noted in parentheses (Table 1), crystals were soaked in the designated soaking solutions for 24−26 h before X-ray data collection, and data collection typically lasted about 25 h.

Data Collection and Structure Refinements. X-ray diffraction data were collected on a multiwire area detector (Hamlin, 1985) (San Diego Multiwire Systems) with monochromatized CuKα radiation (Rigaku RU200 rotating-anode X-ray generator), and intensity observations for each data set were processed with a local UCSD Data Collection Facility software package (Howard et al., 1985). Difference Fourier methods [$F_{o(soak)} - F_{o(native)}$, $\alpha_{c(native)}$], where native refers to the structures that resulted when 6bp and 7bp crystals had been soaked in artificial mother liquor alone (Table 1), were utilized to generate initial electron density maps for the structure determinations of the nucleotide-soaked crystals. After modeling, subsequent least-squares refinement steps were carried out with the TNT program package (Tronrud et al., 1987), in which all reflections from 20 Å to the maximum resolution were included in the calculations. As a part of the TNT program package, a scaling function was applied during refinements to compensate for a lack of solvent continuum in the model for the low-order reflections (Moews & Kretsinger, 1975). Individual isotropic temperature factor refinements were carried out with restrained correlation for bonded atoms. No constraints were placed on metal ion interactions with other

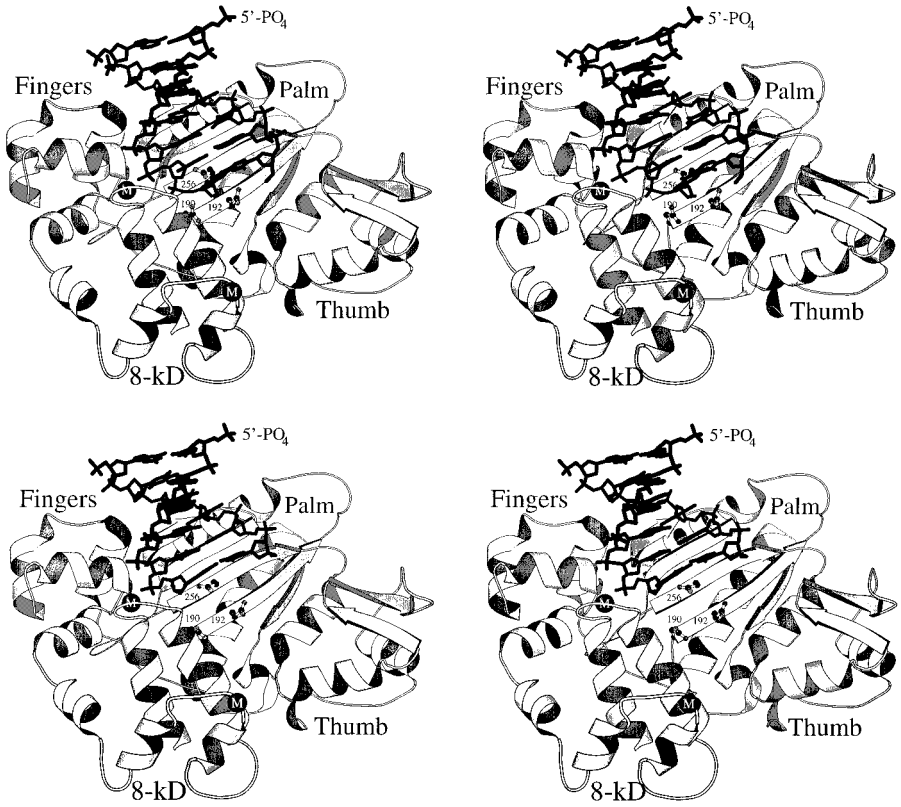

FIGURE 2: SETOR stereo diagrams (Evans, 1993) highlighting the most critical difference between two human DNA pol β-DNA cocrystal structures (Pelletier et al., 1996); the structure in the top panel of human pol β complexed with 7 base pairs of double-stranded DNA (termed the 7bp complex) differs from the structure in the bottom panel of human pol β complexed with 6 base pairs of double-stranded DNA (termed the 6bp complex) by one additional base pair at the active site. Consequently, only the 7bp structure has a reactive primer 3′-OH group positioned at the active site, readily available for catalysis. Pol β comprises an amino-terminal 8-kDa domain and a carboxy-terminal 31-kDa domain, and we have adopted a common nomenclature for polymerase structures (Ollis et al., 1985; Kohlstaedt et al., 1992) in which, because of the resemblance to a hand, the three subdomains of the 31-kDa domain are termed fingers, palm, and thumb (Sawaya et al., 1994). This view looks down into the DNA binding channel so that the palm subdomain, which houses the conserved active-site carboxylate groups (aspartic acids 190, 192, and 256) lies beneath the DNA. Although the sequences of the DNA substrates in the human pol β-DNA binary complexes in the top and bottom panels differ from one another (Pelletier et al., 1996) and also differ from the DNA sequence in the rat pol β−DNA−ddCTP ternary complexes (Pelletier et al., 1994), the DNA is nevertheless bound to pol β in the same way in all three complex structures. The only significant difference between the human pol β−DNA binary complexes shown here and the rat pol β−DNA−ddCTP ternary complexes is a change in the position of the thumb subdomain from an open to a closed conformation, respectively (Pelletier et al., 1996). Metals in the HhH metal sites are depicted as black spheres and are thought to be Na^+ ions for all structures reported here (Pelletier & Sawaya, 1996). For a more detailed characterization of the HhH motifs in pol β, see Pelletier et al. (1996) and Pelletier and Sawaya (1996).

atoms, and no hydrogen-bonding restraints were applied to the DNA base pairs, which may account for the slight differences that were sometimes observed in the DNA structures reported here, particularly at the blunt ends where the *B*-factors were typically larger. The final structures listed in Table 1 have good geometry, with root-mean-square (rms) deviations in bond lengths and bond angles less than or equal to 0.020 Å and 3.0°, respectively.

It should be noted that one of us (H.P.) carried out the crystal soaking, data collection, and data reduction steps, while a second person (M.R.S.) calculated, and subsequently interpreted, the difference Fourier maps with little or no prior knowledge as to what had been soaked into the crystal. With this technique, which eliminated as much bias as possible from the interpretation of the difference Fourier maps, only the results from two crystals that had been soaked in the presence of sulfate ions (Table 1) had to be changed from their original interpretations. For these crystals, electron density near the active site was originally interpreted to be a phosphate group from a poorly bound nucleotide. However, as described below, by analogy with a sulfate ion binding site that has been observed in other pol β crystals structures, we have since reinterpreted this electron density to represent a sulfate ion instead.

RESULTS AND DISCUSSION

Mutagenicity of Mn^{2+}. Solution studies show that Mg^{2+} ions do not bind as strongly to carboxylate groups (Martin, 1990) nor to the triphosphate moiety of nucleotides (Martin, 1990; Smith et al., 1991) as do transition metal ions such as Co^{2+}, Cr^{3+}, Cu^{2+}, Mn^{2+}, Ni^{2+}, or Zn^{2+}. The binding of a nucleotide in the active site of pol β is therefore expected to differ if Mg^{2+}, which coordinates carboxylate groups in the active site as well as nucleotide phosphates (Figure 1), is replaced by a transition metal ion, and as discussed above, such a difference in binding may contribute to the decrease in nucleotide selectivity that is observed for most polymerases in the presence of a metal ion mutagen such as Mn^{2+}. In order to test whether or not we could detect any changes in nucleotide binding in the active site of pol β when Mg^{2+} is replaced by Mn^{2+}, one human pol β−DNA binary complex crystal was soaked in a solution containing 1 mM dATP and 5 mM $MgCl_2$, while a second crystal was soaked in a solution containing 1 mM dATP and 5 mM $MnCl_2$ (Table 1). We had not anticipated at the outset of our

Table 1: Data Collection, Refinement Statistics, and Extent of Reaction in the Crystals

soaking conditions[a]	PDB[b] code	d_{min} (Å)	$\langle I/\sigma_I \rangle$[c]	completeness (%)	R_{sym}[d] (%)	final R[e] (%)	extent of reaction[f]	metal ion observed?[g] catalytic	metal ion observed?[g] nucleotide
native, natural mother liquor	9ICJ[2]	3.1	1.8	88	5.6	14.9	na	no	no
native, artificial mother liquor	8ICB	3.1	1.8	93	6.0	15.3	na	no	no
5 mM $MnCl_2$, 1 mM dATP	8ICR[3]	2.9	2.0	84	4.9	16.1	complete	yes	yes
5 mM $MnCl_2$, 1 mM dATP[h]	8ICP	2.9	2.2	84	4.7	16.6	complete	no	yes
5 mM $MgCl_2$, 1 mM dATP	8ICG	3.3	2.1	93	6.6	14.0	none	no	no
50 mM $MgCl_2$, 10 mM dATP	8ICF[3]	2.9	1.8	94	5.1	18.3	none	no	no
5 mM $MnCl_2$, 5 mM $MgCl_2$, 1 mM dATP	8ICK	2.7	2.3	82	4.0	17.2	complete	yes	yes
0.5 mM $MnCl_2$, 0.1 mM dATP	8ICQ	3.0	1.9	91	5.4	15.9	none	no	no
5 mM $MnCl_2$, 1 mM dATP, 75 mM $(NH_4)_2SO_4$[i]	8ICM	2.9	1.8	94	4.8	17.3	none	no	no
5 mM $MnCl_2$, 1 mM dATP, 75 mM Li_2SO_4[i]	8ICZ	3.1	2.0	94	5.7	15.5	none	no	no
5 mM $CaCl_2$, 1 mM dATP	8ICA	3.0	1.9	90	6.3	15.8	none	no	yes
1 mM $CdCl_2$, 1 mM dATP[j]	8ICE	3.2	1.8	90	7.7	17.0	complete	no	yes
5 mM $CoCl_2$, 1 mM dATP	9ICB	3.2	2.0	93	5.9	15.1	none	yes	yes
5 mM $CrCl_3$, 1 mM dATP	9ICC	3.1	1.8	92	6.5	15.7	none	no	yes
0.1 mM $CuCl_2$, 1 mM dATP[j]	9ICE	2.8	2.0	90	5.0	18.6	none	no	no
5 mM $NiCl_2$, 1 mM dATP	8ICL[3]	3.1	1.8	95	5.4	16.4	none	yes	yes
1 mM $ZnCl_2$, 1 mM dATP[j]	9ICF[3]	3.0	2.0	84	5.7	16.2	partial	no	yes
0.2 mM $ZnCl_2$, 0.1 mM dATP	9ICV	2.7	1.8	90	3.7	17.8	complete	yes	yes
0.02 mM $ZnCl_2$, 0.01 mM dATP (3 days)	1ZQT	3.4	2.1	83	7.8	18.0	none	yes	no
5 mM $MnCl_2$, 1 mM dCTP	8ICT[4]	3.1	1.8	94	5.7	16.7	none	yes	yes
5 mM $MnCl_2$, 1 mM dCTP[h]	8ICS	2.9	1.8	87	5.2	16.5	none	yes	yes
5 mM $MgCl_2$, 1 mM dCTP	8ICH	3.3	1.8	93	6.8	17.2	none	no	no
5 mM $MnCl_2$, 1 mM dGTP	8ICV	3.2	2.0	91	6.3	15.9	partial	no	yes
5 mM $MgCl_2$, 1 mM dGTP	8ICI	2.8	1.8	88	4.6	13.5	none	no	no
5 mM $MnCl_2$, 1 mM dTTP	8ICY	3.1	2.0	94	5.9	16.0	partial	no	yes
5 mM $MgCl_2$, 1 mM dTTP	8ICJ	3.2	1.9	93	7.1	15.7	none	no	no
5 mM $MnCl_2$, 1 mM dTTP (5 min)	8ICX	3.0	1.9	91	5.5	16.0	none	yes	yes
5 mM $MnCl_2$, 1 mM dTTP (4 days)	8ICW	3.3	1.9	92	7.5	16.3	partial	no	yes
1 mM $ZnCl_2$, 1 mM dCTP	9ICG	3.0	1.9	87	5.8	16.0	none	yes	yes
1 mM $ZnCl_2$, 1 mM dGTP	9ICH	2.9	2.0	92	4.4	17.3	none	yes	yes
1 mM $ZnCl_2$, 1 mM dTTP	9ICI	3.1	2.0	94	5.9	16.6	complete	yes	no
5 mM $MnCl_2$, 1 mM ddATP	8ICU	3.0	1.8	90	5.6	17.2	partial	yes	yes
5 mM $MnCl_2$, 1 mM ATP	8ICN	2.8	1.9	89	4.3	17.0	partial	no	yes
5 mM $MnCl_2$, 1 mM AZT-TP	8ICO[4]	2.7	1.9	91	4.3	18.0	none	yes	yes
5 mM $MnCl_2$, 1 mM dATPαS[k]	9ICA[4]	3.0	2.1	87	5.7	16.6	none	yes	yes
6bp; native, natural mother liquor	9ICW[2]	2.6	1.8	95	6.3	17.5	na	no	no
6bp; native, artificial mother liquor	9ICK	2.7	2.3	89	3.6	16.5	na	no	no
6bp; 5 mM $MnCl_2$, 1 mM dATP	9ICQ	2.9	1.9	87	4.9	15.2	none	yes	yes
6bp; 5 mM $MnCl_2$, 1 mM dCTP	9ICR	3.0	1.9	88	5.1	15.7	none	yes	yes
6bp; 5 mM $MnCl_2$, 1 mM dGTP	9ICT	3.0	1.9	94	4.3	15.7	none	yes	yes
6bp; 5 mM $MnCl_2$, 1 mM dTTP	9ICU	2.9	1.9	91	4.3	16.2	none	no	yes
6bp; 5 mM $MgCl_2$, 1 mM dTTP	9ICO	2.9	2.0	86	4.6	15.2	none	no	no
6bp; 5 mM $MnCl_2$, 1 mM pyrophosphate	9ICL	2.8	1.8	91	6.0	16.1	none	yes	yes
6bp; 5 mM $MgCl_2$, 1 mM pyrophosphate	9ICP	3.1	1.8	91	7.4	16.5	none	no	no
6bp; 10 mM $MnCl_2$, 10 mM ddCTP	9ICS[5]	2.9	1.9	93	4.4	16.5	none	yes	yes
6bp; 20 mM $MgCl_2$, 20 mM ddCTP	9ICN[5]	3.0	1.8	86	5.2	15.0	none	no	yes

[a] See Experimental Procedures for a description of how soaking solutions were prepared. All data sets were obtained with 7bp crystals (Figure 2) with the exception of the last 11 data sets, which were obtained from crystals that do not have a primer 3′-OH group available for reaction in the active site (Figure 2) and are designated 6bp in the table. [b] Reflection data and coordinate files are available under the Brookhaven Protein Data Bank code name listed for each structure. PDB codes of structures that have corresponding figures in the paper are superscripted with the figure number. [c] Average ratio of observed intensity to background in the highest resolution shell of reflections. [d] $R_{sym} = \sum|I_{obs} - I_{avg}|/\sum I_{avg}$. [e] Final $R = \sum||F_{obs}| - |F_{calc}||/\sum|F_{obs}|$, including all data between 20 Å and the maximum resolution. Some R-factors are relatively low because a refined, high-resolution 6bp or 7bp structure had been utilized as a starting structure for many lower resolution data sets. Refinement of a high-resolution structure against a closely related low-resolution data set results in a lower R-factor than would be expected if phases for the low-resolution structure had been obtained by other means, such as multiple isomorphous replacement (MIR) phasing. See the PDB files for additional statistics and information about refinements. [f] The presence of a phosphate group bound to the 3′ terminus of the primer was taken as evidence that a nucleotidyl transfer reaction had occurred in the crystal, regardless of whether or not the rest of the incorporated dNMP (that is, the sugar or the base moiety) was visible in the electron density maps. The extent of the reaction was categorized as none if no such phosphate was observed (Figure 3, upper right and lower left), partial if the phosphate group was observed but other electron density was present in the active site that possibly corresponded to unreacted dNTP (Figure 3, lower right), and complete if the phosphate group was observed and there was no other density in the active site with the exception of pyrophosphate (Figure 3, upper left). When no nucleotide soaks were performed (native structures), the extent of reaction is marked not applicable (na). [g] We have renamed what was previously designated metal site B (Pelletier et al., 1994) as the catalytic metal ion binding site, and likewise, the previously designated metal site A (Pelletier et al., 1994) is now termed the nucleotide-binding metal ion (Figure 1). [h] In order to check the integrity of the nucleotide stock solutions, as well as to establish reproducibility of results, data for these soaks were collected toward the end of our experiments, after relatively old nucleotide stock solutions had been rethawed and refrozen numerous times over the course of a few months. [i] These crystals had been soaked in the same artificial mother liquor described in Experimental Procedures with the exception that 150 mM NaCl had been replaced by 75 mM $(NH_4)_2SO_4$ or 75 mM Li_2SO_4, respectively. [j] We were forced to utilize lower metal ion concentrations in the case of Cu^{2+}, Cd^{2+}, and Zn^{2+} because these metal ions cross-linked the crystals and caused cracking and disorder at the higher concentrations (see Table 2). [k] The phosphorothioate derivative dATPαS consists of a 50/50 racemic mixture of the *R* and the *S* absolute configurations.

soaking experiments, however, that such a sharp contrast in results would occur; in the presence of $MnCl_2$, complete reaction of dATP with the primer 3′-OH took place directly in the crystals (Figure 3, upper left), whereas in the presence of $MgCl_2$, there was no evidence at all of a reaction. In fact, there was no evidence of a reaction even when a crystal

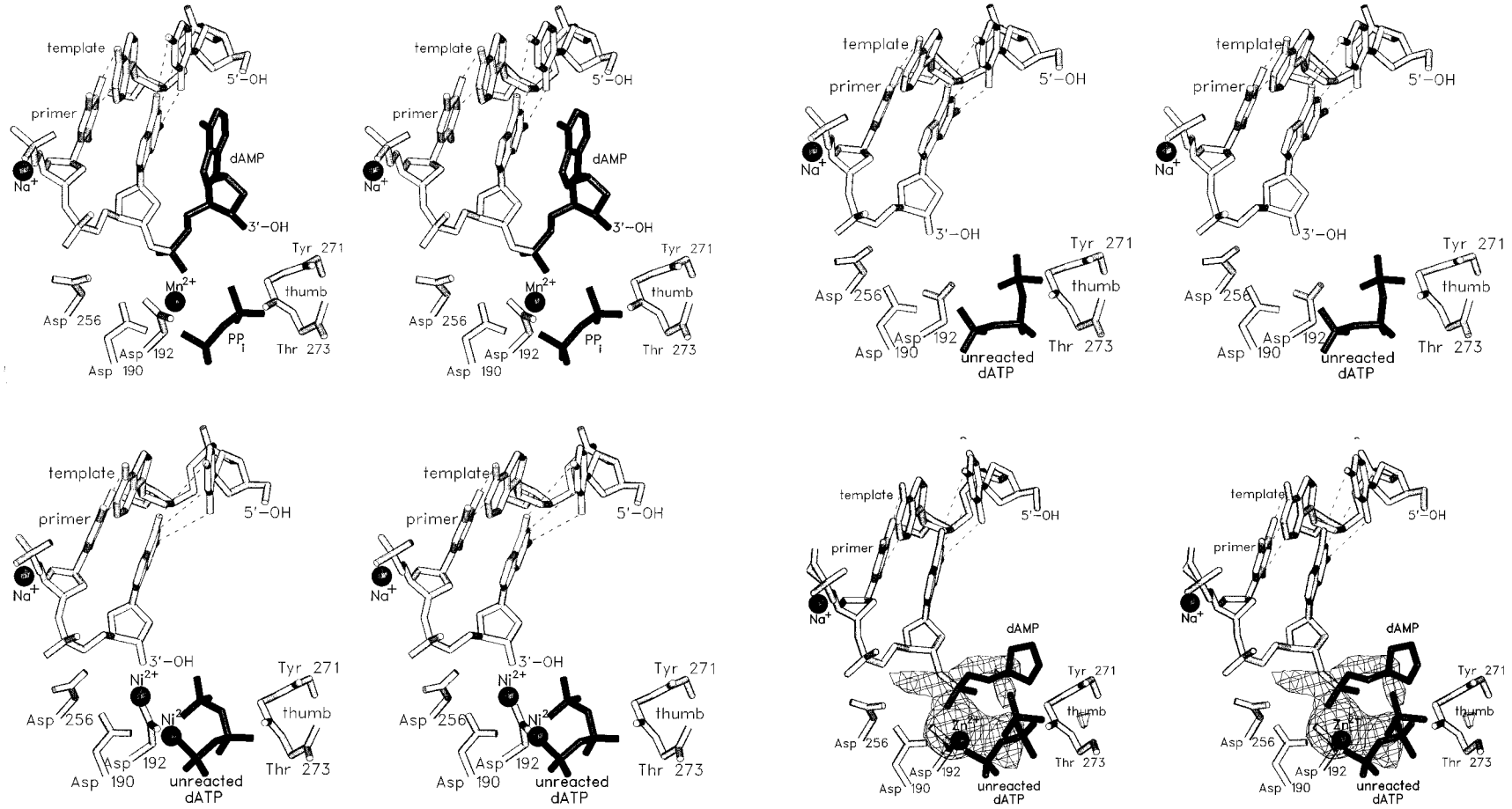

FIGURE 3: SETOR stereo diagrams (Evans, 1993) depicting active sites of human pol β−DNA binary complex crystals that had been soaked for 24−26 h in (upper left) 1 mM dATP and 5 mM $MnCl_2$, showing a complete reaction; (upper right) 10 mM dATP and 50 mM $MgCl_2$, showing no reaction; (lower left) 1 mM dATP and 5 mM $NiCl_2$, once again showing no reaction; and (lower right) 1 mM dATP and 1 mM $ZnCl_2$, showing a partial reaction (Table 1). Darkly shaded portions highlight entities that had been soaked into the crystals. In many cases, the sugar and base moieties of the nucleotide were unobservable in electron density maps and therefore were not modeled into the structure. A sugar-selective backbone segment of the thumb subdomain, tyrosine 271−threonine 273 (Pelletier et al., 1994), is shown to the right of the active sites. In addition, a Na^+ ion from the HhH DNA-binding motif of the fingers subdomain (Pelletier et al., 1996; Pelletier & Sawaya, 1996) has been included in each of the figures. Of all metal ions tested, only Mg^{2+} required higher nucleotide concentrations (10 mM dATP) (Table 1) before the triphosphate moiety could be observed crystallographically, suggesting relatively weak nucleotide binding in the presence of Mg^{2+}. Also, as indicated in the upper right panel, it was difficult to detect Mg^{2+} ions in the active site at this resolution, although they are probably present to some extent. In the upper left panel, the reaction product, Mn^{2+}−pyrophosphate (Mn^{2+}-PP_i), is bound in a manner similar to that observed in the structure of crystals that had been soaked in 5 mM $MnCl_2$ and 1 mM PP_i alone (Table 1). In contrast, no evidence of Mg^{2+}-PP_i binding was observed in the active site of crystals soaked in the presence of 5 mM $MgCl_2$ and 1 mM PP_i (Table 1), once again indicating weaker binding in the presence of Mg^{2+}. That no metal ion is observed in the catalytic metal ion binding site in the upper left panel may be attributed to steric hindrance on the part of the incorporated nucleotide. However, it should be noted that a metal ion has been observed in this site in other soaking experiments that show evidence of a reaction (Table 1), so the underlying cause of why the catalytic metal ion is observed in some structures, but not others, will require further investigation. In the lower left panel, the Ni^{2+} ion coordinates the triphosphate moiety as a α,γ-bidentate, which differs from the β,γ-bidentate that is observed for Mg^{2+} (Pelletier et al., 1994). The active-site geometry of a Co^{2+}−dATP-soaked crystal (Table 1) is indistinguishable from that of the Ni^{2+}−dATP-soaked crystal. In the lower right panel a $F_{o(Zn-dATP)} - F_{o(native)}$, $\alpha_{c(native)}$ difference Fourier map has been superposed on the structure and is contoured at 4σ. Native refers to the 7bp data set collected on a crystal soaked in artificial mother liquor alone (PDB code 8ICB in Table 1). In addition to evidence of a reaction at the 3′-OH primer terminus in the Zn^{2+}−dATP-soaked crystal, subsequent difference Fourier maps during later stages of model building and refinement revealed an unreacted triphosphate moiety in the active site. In that steric hindrance eliminated the possibility that a newly incorporated dATP and an unreacted dATP were present in the same active site, it was assumed that a fraction of the pol β−DNA complexes in the crystal had reacted with the nucleotide to form the product, dAMP, whereas the remaining pol β−DNA complexes in the crystal had unreacted dATP bound in the active site. This has been defined as a partial reaction and has been observed for other nucleotide soaks as well (Table 1). It is suggested that the upper left and lower right panels, in particular, be viewed in stereo so that the difference in the position of the sugar moiety (that is, the difference in reaction products between a mutagen such as Mn^{2+} and a potential mechanism-based inhibitor such as Zn^{2+}) is more apparent.

was soaked at 10 times the Mg^{2+} ion and dATP concentrations utilized in the soaking experiments with Mn^{2+} (Table 1). Only binding of the triphosphate moiety of the nucleotide was observed in the Mg^{2+}-soaked crystals at the higher nucleotide concentration (Figure 3, upper right).

In order to confirm that catalysis in the crystal (in the presence of Mn^{2+}) was facilitated specifically by the trio of carboxylate groups in pol β's active site (Figure 1), we repeated the soaking experiments with human pol β−DNA binary complex crystals that do not have a primer 3′-OH group positioned in the active site [designated as 6bp in Figure 2 (bottom)]. No reaction was observed in these crystals under any conditions tested (Table 1).

The DNA in the binding channel of the human pol β−DNA complex structure is blunt-ended at the active site (Figure 2), so there is no template available for base-pairing with an incoming nucleotide. Although it has been shown that many different polymerases, including pol β, are capable of carrying out nucleotide additions on blunt-ended DNA substrates (Clark et al., 1987; Clark, 1988), it was nevertheless somewhat unexpected that a nucleotidyl transfer reaction could take place directly in the crystal because of the conformational constraints placed on the protein and DNA molecules. For example, because the thumb subdomain in the pol β−DNA binary complex structure is in an open conformation (Pelletier et al., 1996), as opposed to the closed conformation as seen in the ternary complexes (Pelletier et al., 1994), we had assumed that movement of the thumb from the open to the closed conformation, which should position a nucleotide closer to the primer, was a requirement for reaction (crystal packing interactions suggest that the thumb subdomain is locked in an open conformation in the crystals, and any movement of the thumb would probably result in cracked or damaged crystals, which we did not observe during our crystal soaking experiments).

Results from our initial soaking experiments therefore offer some insight into how a metal ion such as Mn^{2+} could act as such a potent mutagen for polymerases. The mechanism that pol β employs for nucleotide selectivity seems to utilize both a bent DNA template and a flexible thumb subdomain (Pelletier et al., 1996), and the sensitivity of the mechanism probably depends strongly on the kinetic, or ligand-exchange, properties (for catalysis) as well as on the electrostatic properties (for nucleotide-binding) of a small, biologically prevalent divalent metal ion such as Mg^{2+}. In contrast, the relatively tightly binding, more reactive Mn^{2+}, which undergoes ligand exchange about 100 times faster than Mg^{2+} (Eigen, 1963; Margerum et al., 1978), appears to be capable of bypassing the sensitive mechanisms of nucleotide discrimination that pol β has developed, and with Mn^{2+} ions in the active site, nucleotidyl transfer apparently can be carried out at random, without the need for instructions from a template and without the need of a closed thumb. These conclusions are in agreement with results from steady-state kinetic experiments with *E. coli* DNA polymerase I, where an increase in the catalytic rate for insertion of mismatched nucleotide substrates was observed when Mg^{2+} was replaced by Mn^{2+} (El-Deiry et al., 1984, 1988). Additional evidence that Mn^{2+} acts as a highly reactive mutagen comes from the observation that Mn^{2+}-dependent activity in the crystal does not appear to be strongly inhibited by the presence of Mg^{2+}; no difference was observed in the extent of the reaction when 5 mM $MgCl_2$ was added to a soaking solution of 5 mM $MnCl_2$ and 1 mM dATP (Table 1).

Physiological Relevance. As pointed out by the 19th century French physiologist, Claude Bernard (Bernard, 1927), one of the greatest challenges facing the medical sciences is the extrapolation of data from in vitro studies to what might be expected to occur in vivo. On the basis of in vitro studies, six of the nine metal ions included in our study (Cd^{2+}, Co^{2+}, Cr^{3+}, Cu^{2+}, Mn^{2+}, and Ni^{2+}) (Table 1) have been categorized as mutagens, and potential carcinogens, because they decrease the fidelity of DNA synthesis (Sirover & Loeb, 1976a). Then again, all of the metal ions in our study except Mg^{2+} and Ca^{2+} are considered trace elements because they occur at such low concentrations in vivo [less than 1 μg/g of tissue in the human body (Versieck & Cornelis, 1989)].[4] In addition, with the possible exception of Cd^{2+}, all of the metal ions in our study are also considered essential for human nutrition (Versieck & Cornelis, 1989). Special care therefore has to be taken when discussing the mutagenicity, and potential carcinogenicity, of a particular metal ion such as Mn^{2+} because a metal ion that proves to be a potent mutagen at relatively high concentrations in vitro may in turn be the cause of malnutrition and disease if not present in sufficiently high concentrations in vivo. Also, it should be kept in mind that, in addition to directly affecting replication and/or repair polymerases, metal ions may act as mutagens and potential carcinogens through other modes of action, such as the induction of oxidative DNA damage (Hartwig, 1995).

Our new experimental system, which is sensitive to a change in the crystal soaking solution from Mg^{2+} to Mn^{2+}, offered an unusual opportunity to study the effects that various other metal ions have on nucleotide binding and catalysis in pol β, but before extensive nucleotide soaking experiments were carried out at the same relatively high (5 mM) metal ion concentrations, an attempt was made to decrease the concentration of Mn^{2+} in the soaking solution to a level that would more closely mimic physiological conditions. Since, however, it is not clear exactly what would constitute physiological conditions, we chose to try a decrease in the nucleotide and metal ion concentrations to one-tenth of those in the original soaking experiments (to 0.1 mM dATP and 0.5 mM $MnCl_2$—though 0.5 mM $MnCl_2$ would probably still not be considered physiological under any circumstances). No reaction was observed under these conditions (Table 1). Although this result precludes an extrapolation of our results to the effect of Mn^{2+} in vivo, it should be noted that if even a small fraction of the active sites in the crystal, which is made up of an estimated 10^{14} pol β molecules, engaged in indiscriminate nucleotidyl transfer in the presence of Mn^{2+}, this would still implicate Mn^{2+} as a powerful mutagen by DNA replication fidelity standards, even though we would not be able to detect such a phenomenon crystallographically.

[4] Much effort has gone into obtaining highly accurate measurements of trace element concentrations in human blood or serum (Versieck & Cornelis, 1989), but it has proven to be more difficult, due to sample collection problems, to measure trace element concentrations within a cell or, even more challenging, within a cell's nucleus, where pol β is located. Even when accurate measurements are made, concentrations are typically reported, by necessity, as the total mass of a given trace element divided by grams of protein or body tissue and not as free metal ion concentrations in solution. What is known, however, is that free metal ion concentrations of trace elements are most likely tightly regulated in vivo by special metal ion binding proteins such as serum albumin or metallothionein, and concentrations may vary considerably, even within the nucleus of a cell (Versieck & Cornelis, 1989).

Although the metal ion and nucleotide concentrations in our experiments cannot be considered physiological, we nevertheless tried to mimic physiological ionic strength conditions as closely as possible by performing all soaks in 150 mM NaCl (Table 1). The importance of the type of salt utilized became apparent when crystal soaking experiments were carried out in solutions in which 150 mM NaCl was replaced by 75 mM $(NH_4)_2SO_4$ or 75 mM Li_2SO_4 (Table 1). Under these conditions no reaction was observed in the crystals, and the only electron density visible in the active site was attributed to a sulfate binding site that has also been observed in 31-kDa crystals grown under high $(NH_4)_2SO_4$ concentrations (Sawaya et al., 1994) or in native 6bp crystals grown in the presence of Li_2SO_4 (Pelletier et al., 1996). Our observations suggest that even low sulfate concentrations can have a large inhibitory effect on nucleotide binding and catalysis for polymerases, in agreement with reports that $(NH_4)_2SO_4$ decreases the rate of DNA synthesis in vitro (Sirover & Loeb, 1976a). In fact, hindsight suggests that, because the previously reported pol β ternary complex crystals grew from a solution containing 75 mM Li_2SO_4 (Pelletier et al., 1994), it is likely that most of the chemical reaction required for crystal formation (where ddCMP was incorporated onto a primer terminus) had occurred before crystallization trays were set up—that is, during the 2-h incubation period before the pol β−DNA−ddCTP reaction sample was exposed to the 75 mM Li_2SO_4 of the crystallization medium. In addition, that sulfate ions may inhibit nucleotide binding also suggests that most of the pol β ternary complexes in the crystallization sample may have been irreversibly locked in a closed conformation, with the ddCTP substrate already tightly bound in the active site, before crystallization trays were set up with Li_2SO_4 (Pelletier et al., 1994).

The presence of sulfate ions in the crystallization medium may have caused problems in the interpretations of phosphate binding behavior in crystal structures of other enzymes as well. A recent example is provided by the enzyme glyceraldehyde-3-phosphate dehydrogenase, where the discovery of a new position for the inorganic phosphate binding site was attributed to a lack of interference from sulfate ions in the crystallization medium (Kim et al., 1995). In addition, the presence of sulfate ions in the soaking solutions may have affected nucleotide binding behavior in previous crystal soaking experiments with pol β (Sawaya et al., 1994) as well as with the Klenow fragment of *E. coli* DNA polymerase I (Beese et al., 1993).

Effects of Ca^{2+}, Cd^{2+}, Co^{2+}, Cr^{3+}, Cu^{2+}, Ni^{2+}, and Zn^{2+} on Nucleotide Binding and Catalysis. The catalytic metal ion binding site in pol β displays a great deal of selectivity when Mn^{2+} is replaced in the soaking solution by other metal ions such as Ca^{2+}, Cd^{2+}, Co^{2+}, Cr^{3+}, Cu^{2+}, Ni^{2+}, or Zn^{2+}. In fact, as discussed below, Zn^{2+} and Cd^{2+} were the only other metal ions, besides Mn^{2+}, that showed evidence of a reaction in the crystals (Table 1). It is not obvious why crystals soaked in the presence of dATP and either Co^{2+} or Ni^{2+}, both of which are similar to Mn^{2+} in certain thermodynamic properties (da Silva & Williams, 1991) and both of which have been characterized as polymerase activators (Sirover & Loeb, 1976b), showed no evidence of a reaction. Clear electron density could be observed for two metal ions and the triphosphate group of the nucleotide, all poised for reaction with the primer 3′-OH group, for both structures (Figure 3, lower left). That there was no reaction under these conditions suggests that perhaps the kinetic properties of the metal ion may be a dominant factor in determining whether or not a reaction occurs. In support of this view, Co^{2+} and Ni^{2+} have relatively slow ligand-exchange rates [slightly slower than Mg^{2+} (Eigen, 1963; Margerum et al., 1978)] when compared with the ligand-exchange rates of Mn^{2+}, Zn^{2+}, or Cd^{2+}, the only three metal ions that gave evidence for a reaction in the crystals. Our observations therefore suggest that, although classified as mutagens (Sirover & Loeb, 1976a) and polymerase activators (Sirover & Loeb, 1976b), Co^{2+} and Ni^{2+} are not very reactive in the catalytic site, and Co^{2+} and Ni^{2+} may instead manifest their mutagenic effects primarily by distorting nucleotide binding, as is indicated by the abnormal α,γ-bidentate coordination geometry that is observed for these metal ions in their interactions with the triphosphate moiety of dATP (Figure 3, lower left).

Cr^{3+} was also incapable of carrying out catalysis in the crystals (Table 1), but in this case electron density in the active site was difficult to interpret and gave some evidence of a greatly distorted Cr^{3+}−triphosphate interaction, which was possibly the result of the higher oxidation state of the trivalent Cr^{3+} ion. In addition, only the nucleotide-binding metal ion was observed, with no evidence of any Cr^{3+} bound in the catalytic metal ion site (Table 1), indicating that the catalytic metal ion binding site in pol β may be selective for divalent metal ions only.

Distorted triphosphate binding of a different kind was observed in the presence of Ca^{2+}, which also showed no evidence of reaction (Table 1). Only the β- and γ-phosphates of the nucleotide could be observed in the active site, and although somewhat similar to the β,γ-bidentate binding observed with Mg^{2+}−ddCTP (Pelletier et al., 1994), the bond distances between Ca^{2+} and the phosphate oxygens are much longer (about 3.5 Å). Like Cr^{3+}, Ca^{2+} also showed no evidence of binding in the catalytic metal ion site, but because Ca^{2+} was the largest divalent metal ion tested, this result was taken as evidence that the catalytic metal ion binding site in pol β, in addition to being valence-specific, is probably size-specific as well.

Despite reports that Cu^{2+} has a ligand-exchange rate that is comparable to that of Mn^{2+}, Cd^{2+}, and Zn^{2+} (Eigen, 1963; Margerum et al., 1978), no reaction was observed in the crystals when soaked in the presence of Cu^{2+} and dATP. This may be due to the fact that a relatively low Cu^{2+} concentration (0.1 mM) had to be utilized in the soaking experiment (Table 1). Pol B−DNA cocrystals were particularly sensitive to higher Cu^{2+} concentrations, and by analogy with somewhat less extreme yet similar behavior observed during soaking experiments with Zn^{2+} and Cd^{2+}, we attribute the sensitivity to intermolecular cross-linking in the crystals. An intermolecular contact site in the crystal lattice between histidine 51 of one pol β molecule and histidine 134 of a symmetry-related pol β molecule forms a good binding site for Cd^{2+}, Cu^{2+}, and Zn^{2+}, all three of which coordinate to both histidines similarly in the crystals. At concentrations of 0.1 mM or higher, this results in cross-linked crystals that crack during the soaking experiments, diffract relatively poorly, differ in unit cell lengths, and are also somewhat more sensitive to X-rays (Tables 1 and 2). It is interesting to note that Zn^{2+} induces higher order aggregates in pol β (Kim et al., 1994), and the intermolecular cross-linking observed in the crystal may represent an intermolecular cross-linking site in solution.

Table 2: Data Collection and Refinement Statistics for Crystals Soaked in Low-Concentration Metal Ion Solutions (No Nucleotides Included)

soaking conditions[a]	PDB Code	d_{min} (Å)	$\langle I/\sigma \rangle$[b]	completeness (%)	R_{sym}[c] (%)	final R[d] (%)	metal ion in catalytic site?	torsion angles[e] (°) Asp190	Asp192	Asp256
7bp; native, natural mother liquor	9ICJ	3.1	1.8	88	5.6	14.9	no	53	−146	−53
7bp; native, artificial mother liquor	8ICB	3.1	1.8	93	6.0	15.3	no	50	−153	−59
7bp; 5 mM $MnCl_2$, 1 mM dCTP	8ICT	3.1	1.8	94	5.7	16.7	yes	50	−44	−55
native, natural mother liquor	9ICW	2.6	1.8	95	6.3	17.5	no	47	−153	−63
native, artificial mother liquor	9ICK	2.7	2.3	89	3.6	16.5	no	46	−158	−52
0.1 mM $CaCl_2$ (3 days)	7ICE	2.8	2.0	90	4.6	16.2	no	46	−100	−59
0.1 mM $CdCl_2$[f]	7ICU	3.3	1.9	89	6.4	16.5	no	52	−160	−65
0.1 mM $CdCl_2$ (4 days)[f]	7ICF	3.1	1.9	93	6.3	15.8	yes	36	41	−63
0.01 mM $CdCl_2$	7ICG	3.0	1.8	94	5.6	15.9	no	56	−163	−61
0.1 mM $CoCl_2$	7ICH	2.9	2.2	85	5.1	15.4	no	44	−171	−62
0.1 mM $CrCl_3$	7ICI	2.8	2.0	85	4.7	15.5	no	45	−161	−57
0.1 mM $CuCl_2$[f]	7ICJ	3.5	1.8	92	8.8	16.3	no	36	−46	−72
0.1 mM $MgCl_2$	7ICK	2.9	2.3	91	4.8	15.2	no	52	−150	−58
0.1 mM $MnCl_2$	7ICL	3.1	1.8	92	7.2	15.6	no	36	−165	−64
0.1 mM $MnCl_2$, no NaCl (2 days)[g]	7ICV	2.8	1.8	89	5.5	16.3	no	45	−15	−62
1.0 mM $MnCl_2$	7ICM	3.0	1.8	94	5.8	15.2	no	46	−168	−51
0.1 mM $NiCl_2$ (4 days)	7ICN	2.8	2.1	89	3.4	16.2	no	48	−161	−55
1.0 mM $ZnCl_2$ (3 days)[f]	7ICR	3.0	1.9	92	5.2	16.0	yes	87	−9	−61
0.1 mM $ZnCl_2$[f]	7ICO	3.3	2.0	91	7.5	15.6	no	41	−167	18
0.1 mM $ZnCl_2$ (4 days)[f]	7ICQ	2.9	2.0	92	4.5	15.9	yes	42	−161	−59
0.01 mM $ZnCl_2$[f]	7ICP	3.0	1.9	94	5.4	15.7	yes	34	50	−54
0.01 mM $ZnCl_2$, 1 mM $MgCl_2$ (3 days)[f]	7ICT	2.8	1.9	92	4.2	16.8	no	41	−100	−62
0.001 mM $ZnCl_2$	7ICS	2.8	1.8	83	4.4	19.6	no	42	−155	−67

[a] See Experimental Procedures for a description of how soaking solutions were prepared. The first five data sets listed are from Table 1 and are included here so that torsion angles for the conserved active-site aspartic acid residues can be compared. With the exception of the first three data sets, which are designated 7bp because they derive from 7bp crystals, all data sets were obtained with 6bp crystals (Figure 2). [b] Average ratio of observed intensity to background in the highest resolution shell of reflections. [c] $R_{sym} = \sum|I_{obs} - I_{avg}|/\sum I_{avg}$. [d] Final $R = \sum|F_{obs} - F_{calc}|/\sum F_{obs}$, including all data between 20 Å and the maximum resolution. [e] Torsion angles are defined by four atoms of each aspartic acid residue (N and Cα of the backbone and Cβ and Cγ of the side chain), and they represent the angle made between the N−Cα bond and the Cβ−Cγ bond when looking down the Cα−Cβ bond axis. [f] An intermolecular contact site in the crystal lattice between histidine 51 of one pol β molecule and histidine 134 of a symmetry-related pol β molecule forms a good binding site for Cd^{2+}, Cu^{2+}, and Zn^{2+}, resulting in cross-linked crystals that cracked during the soaking experiment and were sensitive to X-ray during data collection. We have discovered that somewhat better diffraction data can be obtained, at least for Cd^{2+} and Zn^{2+}, if crystals are soaked for a few days, rather than the standard 24−26 h, probably because they are allowed some time to anneal. This is evidenced by the fact that many of the cracks observed during the initial soaking period were usually completely gone after a day or two. [g] The artificial mother liquor for this crystal differed from the standard artificial mother liquor only in that in lacked 150 mM NaCl. Although no metal ion was observed in the catalytic site for this structure, a change in the torsion angle for aspartic acid 192 to −15° indicates that a Mn^{2+} ion may be present at low occupancy. If this is the case, our results also suggest that NaCl slightly inhibits metal ion binding in the catalytic site, because no such change in torsion angle was observed for aspartic acid 192 when a similar soaking experiment was carried out in the presence of 150 mM NaCl (compare with data set listed just above this data set).

In addition to displaying similar cross-linking behavior, Cd^{2+}, Cu^{2+}, and Zn^{2+} were the only three metal ions capable of inducing a large change in the torsion angle of Asp 192 at relatively low (0.1 mM) concentrations (Table 2), suggesting that Cu^{2+}, like Cd^{2+} and Zn^{2+}, might cause an observable reaction in the crystal if it could be tested at a slightly higher concentration. It is common for Cd^{2+}, Cu^{2+}, and Zn^{2+} to display similar binding behavior, as is demonstrated with the Zn^{2+}-regulating protein metallothionein (MT), which also binds all three metal ions similarly (Braun et al., 1992)—although in this case, the metal ions are coordinated to cysteine residues rather than to histidines or to carboxylates.

Results obtained with nucleotide soaks in the presence of Zn^{2+} are particularly interesting because, unlike Mn^{2+}, a reaction was observed in the crystals even when Zn^{2+} and dATP concentrations were decreased to 0.2 and 0.1 mM, respectively (Table 1). Although these are still not considered physiological concentrations (Versieck & Cornelis, 1989; Williams, 1989), Zn^{2+} is nevertheless the most reactive essential metal ion that we tested, suggesting a potential role for Zn^{2+} in pol β's function in vivo [Cd^{2+} was relatively reactive as well (Table 1), but Cd^{2+} is not considered an essential element (Versieck & Cornelis, 1989)]. In fact, of all the metal ions tested, the catalytic metal ion binding site in pol β has the strongest affinity for Zn^{2+}, which shows evidence of binding even at concentrations as low as 0.01 mM (Table 2). Additional evidence that Zn^{2+} may play a role in pol β's function in vivo is provided by the observation that the reaction product for Zn^{2+} differs from that of Mn^{2+} (Figure 3, upper left and lower right); in the case of Mn^{2+}, the newly incorporated, covalently bound dAMP at the primer terminus has taken on the structure and geometry of its B-DNA surroundings, just as if there were a template present for proper base-pairing (Figure 3, upper left), whereas in the case of Zn^{2+}, although the base is not observed in the crystal structure, the sugar moiety of the incorporated dAMP protrudes into the solvent, away from the primer terminus (Figure 3, lower right). Therefore, unlike reaction products obtained in the presence of Mn^{2+}, reaction products in the presence of Zn^{2+} suggest that polymerization has reached a dead end and cannot continue. Our observations are in agreement with the categorization of Zn^{2+} as a polymerase inhibitor (Sirover & Loeb, 1976a) rather than as a mutagen like Mn^{2+}.

Another noteworthy reaction product that resulted from the nucleotide-soaking experiments in the presence of $ZnCl_2$ was observed in the case of the Zn^{2+}−dTTP soak (Table 1). In this case, the only density visible in the active site corresponded to the monophosphate group of a newly incorporated dTTP, suggesting that the sugar and base moieties might have been cleaved away in the reaction, possibly with the help of the Zn^{2+} ion. A similar reaction product was observed with Cd^{2+} in the presence of dATP,

albeit no Cd^{2+} was observed in the catalytic site (Table 1), offering further support for the idea that the catalytic metal ion binding site in pol β may select against the size of the metal ion (although, in this case, size did not prevent catalysis). All of our results suggest a possible regulatory role for Zn^{2+} in pol β's function in vivo. For example, it is possible that an exonuclease such as DNase V, which is thought to be associated with pol β's repair functions in vivo (Mosbaugh & Meyer, 1982; Mosbaugh & Linn, 1983), may serve to cleave off the distorted, seemingly inhibitory Zn^{2+}−3′-PO_4 group, thus freeing pol β, as well as the primer terminus, for further reaction. Although the idea of Zn^{2+} serving a possible regulatory role in pol β's functions in vivo is based on preliminary structural data alone, recent reports that the expression level of the Zn^{2+}-regulating protein metallothionein may be coupled to DNA repair activity in cancer cells (Cherian et al., 1994; Satoh et al., 1994) suggests that a role for Zn^{2+} in pol β's functions in vivo may warrant further investigation.

Nucleotide Selectivity in the Presence of Mn^{2+}: the Base Moiety. Although we have shown that Mn^{2+} promotes non-template-directed nucleotidyl transfer in our crystals (Figure 3, upper right), subtle levels of nucleotide selectivity can nevertheless still be detected in the active site when human pol β−DNA binary complex crystals are soaked in the presence of Mn^{2+} and various nucleotides that differ in either the base, the sugar, or the triphosphate moiety (Table 1; Figure 4). For example, all three nucleotides (dCTP, dGTP, and dTTP), which differ from dATP only in the base moiety, gave noticeably different results when soaked in the presence of 5 mM $MnCl_2$ (Table 1). In the case of dCTP, no reaction was observed at all and only unreacted dCTP could be modeled into the active site (Figure 4, top). In the case of dGTP and dTTP, there was some evidence of a reaction, but after the reaction product, deoxynucleoside monophosphate (dNMP), had been modeled into the electron density, additional density was interpreted to be unreacted nucleotide, indicating a partial reaction like that observed in the Zn^{2+}−dATP-soaked crystal described above (Table 1; Figure 3, lower right). In that, in the case of the Mn^{2+}−dTTP-soaked crystal, there appeared to be relatively more electron density attributable to unreacted nucleotide, it was estimated that the extent of reaction for dTTP was less than that for dGTP. These results agree with observations that dATP was consistently favored over dCTP, dGTP, and dTTP in solution studies where various procaryotic and eukaryotic polymerases, including pol β, were tested for nucleotide additions to blunt-ended DNA substrates (Clark et al., 1987; Clark, 1988).

In an attempt to investigate the partial reaction phenomenon more thoroughly, a short-term dTTP soak (5 min instead of 24 h) was carried out, and the resulting difference Fourier map showed no evidence of a reaction, though bound dTTP was observed in the active site (Table 1). Although this suggests that the differences in extent of reaction observed when the base moiety is varied (dATP, dCTP, dGTP, and dTTP) could be due to slightly different soaking times for each of these nucleotides, two lines of evidence favor the idea that 24 h was sufficient time to allow the full extent of a reaction to be reached, whatever that may be, by the time data collection began for all nucleotide soaking experiments: (i) a 4-day dTTP soak gave results that did not differ significantly from the standard 1-day dTTP soak (Table 1), and (ii) results from the fully reacted dATP (Figure 3, upper right) and the completely unreacted dCTP (Figure 4, top) soaking experiments were reproducible (Table 1). The phenomenon of the partial reaction is therefore still not clear to us and will require further investigation.

As described above, there is no template overhang available for base-pairing in the pol β−DNA crystals (Figure 2), so it is not obvious why results vary so much among nucleotides that differ only in the base moiety. However, since the extent of the reaction in the crystals appears to be coupled to the size of the base moiety (dATP > dGTP > dTTP > dCTP), one possible explanation for our observations is that base-stacking interactions with the terminal nucleotide (dGMP) of the primer in the pol β−DNA binary complex structure selectively stabilizes the larger purine bases (Figure 3, upper right) more than the smaller pyrimidine bases (Figure 4, top), resulting in greater reaction yields for the purines. Further support for the idea that pyrimidines may bind slightly differently from purines is offered by results from nucleotide soaking experiments with crystals that lack the terminal nucleotide of the primer (designated 6bp in Table 1 and Figure 2). In this case, however, it is the smaller pyrimidines (dTTP and dCTP), and not the purines (dATP and dGTP), that seem to display slightly more stable binding. Although binding of the triphosphate group of the nucleotide can be observed for all four nucleotides, the sugar moiety is ordered enough to be observed only in the dTTP and dCTP structures, suggesting greater stability for these nucleotides (the base moiety is too disordered to be observable for all four nucleotides). One possible explanation for these observations is that strong van der Waals and hydrophobic interactions between the sugar moiety of the nucleotide and backbone atoms of the thumb subdomain (Figure 4, top) help to stabilize nucleotide binding in the active site, and such interactions may be more favorable with the less bulky pyrimidines, dCTP and dTTP. The sugar−thumb interactions observed in many of the nucleotide-soaked crystals presented here are similar to the sugar−thumb contacts observed in the closed, ternary complex structures (Pelletier et al., 1994), and their potentially important role in controlling thumb movement during catalysis is discussed in greater detail below.

Selectivity for the Sugar Moiety in the Presence of Mn^{2+} and either ATP, ddATP, or AZT-TP. In view of the intimate contacts that the sugar moiety of the nucleotide makes with the thumb subdomain—even with the thumb in the open conformation—it is perhaps not surprising that soaking experiments with ddATP, ATP, and AZT-TP, all of which differ from their corresponding dNTPs by an addition or a deletion of a particular group on the sugar, displayed somewhat different reactivities in the crystals when compared with their dNTP counterparts, dATP, dATP, and dTTP, respectively (Table 1). In the case of ddATP and ATP, additional electron density in the active site gave evidence for a partially reacted nucleotide that resembled those of the Zn^{2+}−dATP, the Mn^{2+}−dTTP, and the Mn^{2+}−dGTP soaks described above, indicating that the nucleotidyl transfer reaction had been hindered somewhat in the cases of ddATP and ATP, at least when compared with the fully reacted dATP structure (Figure 3, upper right). This type of sugar selectivity in the active site of pol β is perhaps best explained by analogy with the children's story of Goldilocks and the Three Bears, where two sugar hydroxyl groups (2′-OH and 3′-OH) in the case of ATP makes the sugar moiety "too big", and no sugar hydroxyl groups in the case of ddATP makes

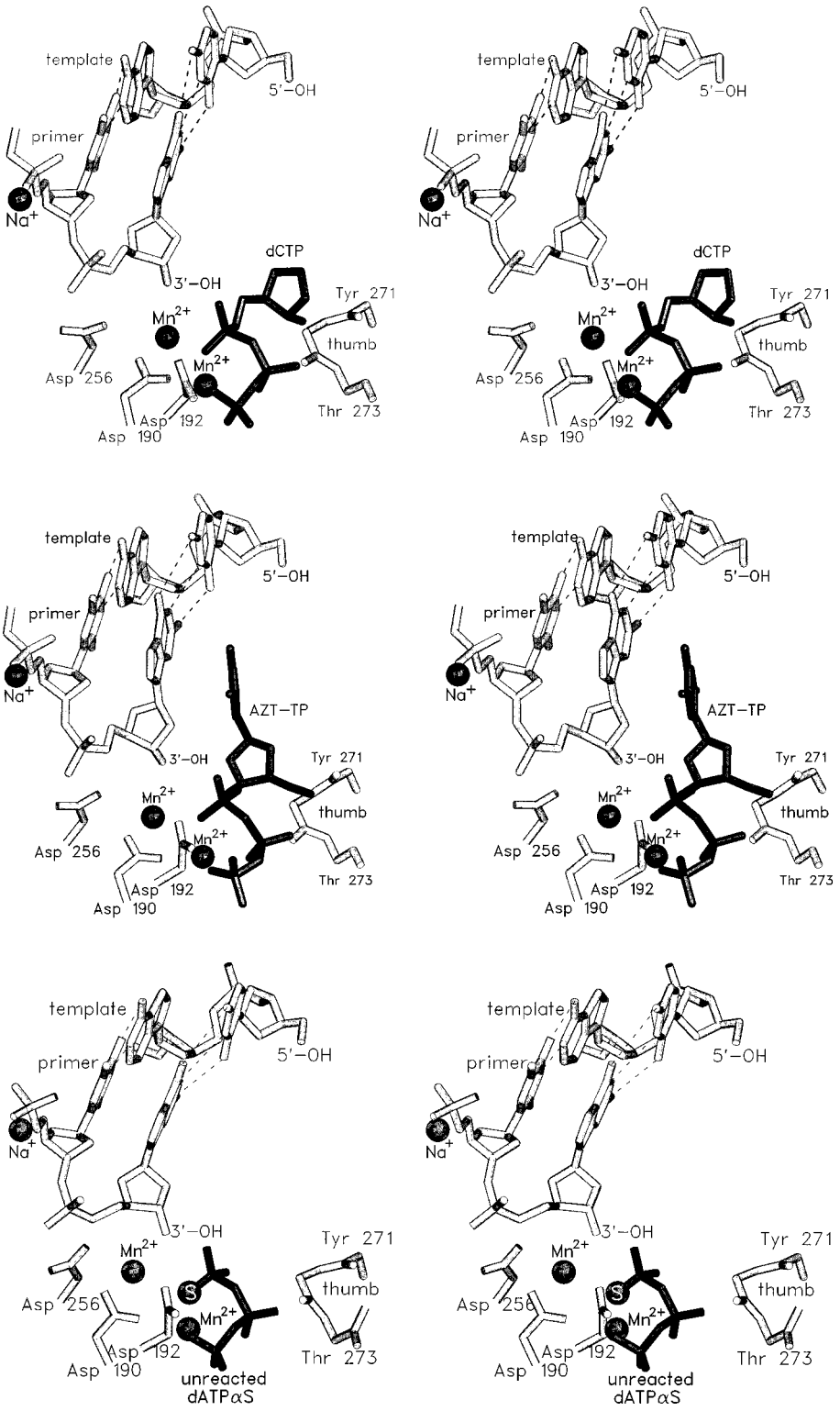

FIGURE 4: SETOR stereo diagrams (Evans, 1993) showing examples of various levels of nucleotide selectivity in the active site of pol β in the presence of Mn^{2+}. The view is the same as in Figure 3. In contrast to crystals soaked in the presence of Mn^{2+} and dATP (Figure 3 upper right), no reaction occurs when crystals are soaked in the presence of Mn^{2+} and either dCTP, AZT-TP, or dATPαS (Table 1), as is evident by the active sites shown in the top, middle, and bottom panels, respectively. These observations indicate that large differences in reactivity can be detected by our experimental system as a result of subtle changes in (top) the base moiety (dCTP), (middle) the sugar moiety (AZT-TP), and (bottom) the triphosphate moiety (dATPαS) of the nucleotide, respectively. In the top panel, the strong hydrophobic and van der Waals contacts between the sugar moiety of dCTP and the backbone atoms of the thumb subdomain were commonly observed throughout our crystal soaking experiments with various metal ions and nucleotides, and such interactions may be responsible for coupling movement of the thumb subdomain with the nucleotide. In the middle panel, the bulky azido group of ATZ-TP protrudes from the 3′ carbon of the sugar moiety and pushes against the backbone atoms of the thumb subdomain. In the bottom panel, relatively strong electron density, which we have interpreted as a sulfur atom, was observed for only one of the two nonbridging α-phosphates, suggesting that, in the presence of Mn^{2+}, pol β favors binding the *R* absolute configuration of dATPαS over the *S* absolute configuration. It should be noted that, in determining the absolute configuration of dATPαS, it was assumed that the sugar moiety, which is too disordered to be observed in the crystal structure, is bound in the active site in a roughly similar fashion as the sugar moieties of the nucleotides in the top and middle panels.

the sugar moiety "too small", but one sugar hydroxyl group (3′-OH) in the case of dATP makes the sugar moiety "just right" for binding and catalysis. In agreement with this analysis, results from the crystal soaking experiment with AZT-TP, in which the bulky azido group makes the sugar moiety especially "too big", showed that no reaction had occurred at all in the crystal (Table 1), and the large distortion in nucleotide binding caused by the azido group is apparent (Figure 4, middle). These results are in agreement with observations that pol β is more sensitive to inhibition by ddNTPs than to inhibition by AZT-TP (Cherrington et al., 1994). Pol β therefore appears to select for the proper size and shape of the sugar moiety, and our results confirm previous proposals that this selectivity process is probably carried out by contacts with the backbone segment of pol β's thumb subdomain between Tyr 271 and Gly 274 (Pelletier et al., 1994) (Figure 4).

Selectivity for the Triphosphate moiety in the Presence of Mn^{2+} and dATPαS. Soaking experiments with the phosphorothioate derivative dATPαS, in which one of the two nonbridging oxygen atoms of the α-phosphate of dATP is replaced with a sulfur atom, shows that the pol β active site is also selective in binding the triphosphate moiety because no reaction was observed in crystals soaked in dATPαS (Table 1; Figure 4, bottom). In addition, although the soaking solution contained a 50/50 racemic mixture of dATPαS (Table 1), pol β appears to favor binding of the *R* absolute configuration of dATPαS as opposed to the *S* absolute configuration, at least in the presence of Mn^{2+} (Figure 4, bottom). Phosphorothioate derivatives are utilized extensively in pre-steady-state kinetic work with polymerases, and the lack of an elemental effect with dATPαS is usually taken as evidence that catalysis is not rate-limiting in the nucleotidyl transfer reaction (Kuchta et al., 1987; Patel et al., 1991; Wong et al., 1991; Spence et al., 1995; Werneburg et al., 1996). Although we are not able to draw any strong conclusions about the effect that dATPαS has on reaction rates in our experimental system, perhaps the binding behavior of dATPαS in pol β can shed some light on an apparent contradiction in the literature concerning the details of the nucleotidyl transfer mechanism (Burgers & Eckstein, 1979; Pelletier et al., 1994).

Many aspects of the proposed nucleotidyl transfer mechanism for pol β (Pelletier et al., 1994) correlated well with conclusions drawn from kinetic work with *E. coli* DNA pol I in the presence of dATPαS (Burgers & Eckstein, 1979), but there was one important exception: although the crystal structure showed that a metal ion (Mg^{2+}) was appropriately positioned in the active site of pol β to stabilize the pentacoordinated α-phosphate of a nucleotide during catalysis (Figure 1), results from kinetic studies with dATPαS indicated that this function was performed by a protein side chain, and specifically not a metal ion (Burgers & Eckstein, 1979). The conclusions of Burgers and Eckstein were based on the idea that if a metal ion coordinates the α-phosphate of a nucleotide in the active site and participates in catalysis, then a noticeable difference in kinetic behavior should be observed with dATPαS when Mg^{2+} (which does not bind sulfur as well as oxygen and therefore should prefer one absolute configuration of dATPαS over the other) is replaced by Mn^{2+} (which is thought to bind oxygen and sulfur with equal affinity and therefore should show no selectivity in binding either configuration of dATPαS).

In agreement with the position of the proposed catalytic metal ion observed in the active site of pol β (Figure 1), kinetic studies had shown that pol I selectively utilizes only the *S*, and not the *R*, absolute configuration of dATPαS in the presence of Mg^{2+} (Burgers & Eckstein, 1979). However, in apparent contradiction to the structural work was the reported observation that pol I also selectively utilizes only the *S*, and not the *R*, absolute configuration of dATPαS in the presence of Mn^{2+} as well (Burgers & Eckstein, 1979). As described above, the fact that no difference in kinetic behavior was observed between Mg^{2+} and Mn^{2+} under these conditions led to the conclusion that a protein side chain, rather than a metal ion, stabilizes the negative charge on the α-phosphate during catalysis (Burgers & Eckstein, 1979). One possible explanation for this anomaly is that, as revealed by our structural studies with dATPαS, it is probably not valid to assume that Mn^{2+} shows no preference for one configuration of dATPαS over another. The strong preference that pol β displays for binding the *R* absolute configuration of dATPαS in the presence of Mn^{2+} (Figure 4C) (although opposite from the strong repulsion that is expected for the *R* absolute configuration of dATPαS in the presence of Mg^{2+}) may stabilize ground-state binding to such an extent that the same net effect is produced with both Mg^{2+} and Mn^{2+}, that is, a significant decrease in catalysis with the *R* absolute configuration of dATPαS.

A Sugar−Triphosphate Binding Pocket in Pol β. All of our observations indicate that pol β's active site possesses several tiers of selectivity for various nucleotides, even in the absence of a template and even with the thumb subdomain in an open position. However, in that many of our observations derive from experiments carried out in the presence of Mn^{2+}, not Mg^{2+}, it is important to determine how much of the nucleotide binding behavior observed with Mn^{2+} may be relevant to pol β's behavior in vivo, where Mg^{2+} is most likely the metal ion utilized for nucleotide binding and catalysis. To this end, some of the most significant differences, as well as important similarities, in the nucleotide-binding properties of Mn^{2+} and Mg^{2+} are demonstrated by results from crystal soaking experiments with ddCTP (Table 1; Figure 5, top and middle panels). Although any nucleotide would have sufficed for Mn^{2+}−Mg^{2+} comparisons, ddCTP was specifically chosen in this case so that subsequent comparisons could be made between the binding of ddCTP in the open-thumbed structure presented here and the binding of ddCTP in the previously reported closed-thumb crystal structure (Pelletier et al., 1994) (Figure 5, bottom). Also, in order to prevent a reaction from occurring at the active site in the presence of Mn^{2+}, 6bp crystals, which do not have a primer 3′-OH group positioned near the catalytic residues (Figure 2, bottom) were utilized for these experiments (Table 1; Figure 5).

As had been observed in many of the soaking experiments with other metal ions and nucleotides (Figures 3 and 4), the two most significant differences between Mn^{2+} and Mg^{2+} are (i) Mn^{2+} coordinates the triphosphate moiety of the nucleotide as an α,γ-bidentate, whereas Mg^{2+} coordinates the triphosphate as a β,γ-bidentate, and (ii) the nucleotide displays much weaker binding in the presence of Mg^{2+} so that a relatively high concentrations of ddCTP was needed before any nucleotide binding (in this case, only the triphosphate moiety) could be observed in the crystal structure (Table 1; Figure 5, top and middle panels). A third, less obvious difference is that the torsion angle of the side

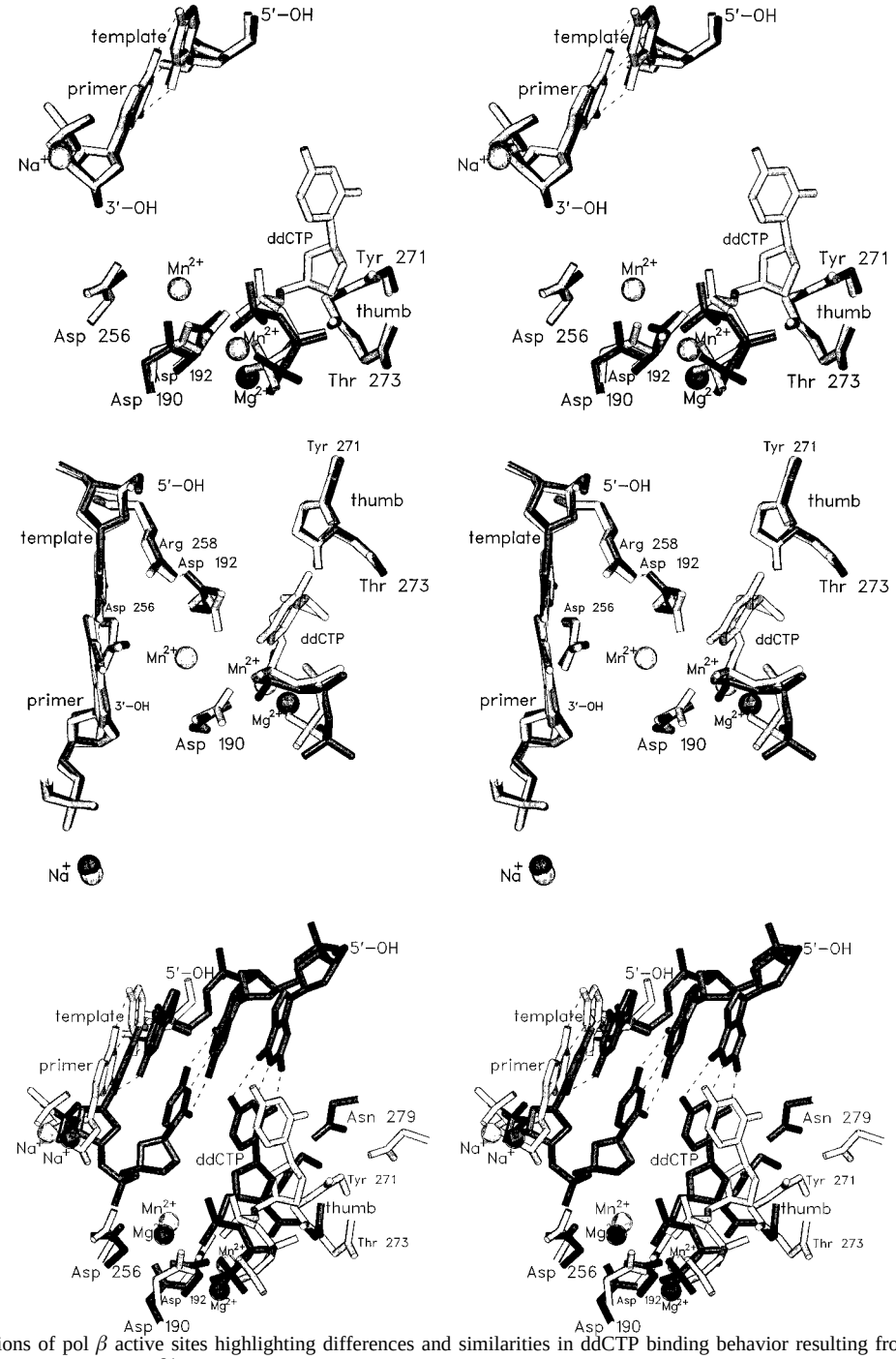

FIGURE 5: Superpositions of pol β active sites highlighting differences and similarities in ddCTP binding behavior resulting from (top) a change in the metal ion from Mn^{2+} (lighter shade) to Mg^{2+} (darker shade) (the middle panel represents a different view of the same superposition) and (bottom) a change in the position of the thumb subdomain from an open conformation (lighter shade) to a closed conformation (darker shade) (Pelletier et al., 1994). The view in the top and bottom panels is the same as in Figures 3 and 4, and the view in the middle panel looks down into the active site and is shown to highlight the change in torsion angle of aspartic acid 192. In the top and middle panels, Mn^{2+} coordinates the triphosphate moiety of the nucleotide as an α,γ-bidentate, whereas Mg^{2+} coordinates the triphosphate as a β,γ-bidentate. In addition, the torsion angle of the aspartic acid 192 side chain differs by almost 180° between the two structures. Because of weaker binding, the Mg^{2+}−ddCTP-soaked crystals required higher ddCTP concentrations than the Mn^{2+}−ddCTP-soaked crystals before nucleotide binding (in this case, only the triphosphate moiety) could be observed crystallographically (Table 1). Although similar soaking experiments, where pol β apoenzyme crystals were soaked in the presence of Mn^{2+} and dATP (Sawaya et al., 1994), revealed a different binding behavior for the nucleotide from that observed here (only the γ-phosphate positions are the same), intermolecular crystal packing interactions between the base of the dATP and a symmetry-related pol β molecule in the asymmetric unit may have interfered with nucleotide binding in the apoenzyme crystals (Sawaya et al., 1994). In addition, sulfate ions in the soaking solution could have inhibited binding of the triphosphate moiety to some extent, as described in the text. Although it would have been desirable in the bottom panel to compare Mg^{2+}−ddCTP binding in the closed-thumb rat ternary complex structure (Pelletier et al., 1994) with an opened-thumb human pol β−DNA binary complex crystal that was soaked with Mg^{2+}−ddCTP rather than with Mn^{2+}−ddCTP, neither the sugar nor the base moieties of our Mg^{2+}−ddCTP-soaked crystal were observable in electron density maps, and as a result, the Mn^{2+}−ddCTP structure was utilized for comparisons in the bottom panel instead. The hydrogen-bond distance between O2 of the ddCTP base moiety and ND2 of asparagine 279 in the bottom panel is 3.0 Å in the closed complex (Pelletier et al., 1994), but this hydrogen bond does not exist in the open structure, with the distance between these two atoms in the open structure being 4.7 Å. In contrast, the distance between C2′ of the ddCTP sugar moiety and the backbone carbonyl oxygen of Tyr 271 remains virtually the same (3.0 and 3.2 Å for the open and the closed structures, respectively), in agreement with the idea that strong sugar−thumb interactions may be a dominant force in determining thumb movement in pol β. That the side chain of asparagine 279 does not appear to initialize thumb movement and that only the backbone atoms of tyrosine 271 seem to perform this function is confirmed by results from fidelity assays (Beard et al., 1996), where results show that amino acid substitutions for neither asparagine 279 nor tyrosine 271 affect nucleotide discrimination for pol β. These stereo diagrams were generated with SETOR (Evans, 1993).

chain of aspartic acid 192 differs by about 130° between the two structures (−179° versus −52° for the Mg^{2+}−ddCTP and the Mn^{2+}−ddCTP structures, respectively) (Figure 5, middle). Aspartic acid 192 is one of three conserved carboxylate residues in the active site of pol β and most likely facilitates metal ion and nucleotide binding during catalysis (Figure 1). In the absence of metal ions and with the thumb subdomain in an open position, the side chain of aspartic acid 192 typically has a torsion angle between −140° and −180° and bends away from the active site to form a strong hydrogen bond with arginine 258 (Figure 5, middle). However, in the presence of relatively high concentrations (~5 mM) of all of the metal ions tested except Mg^{2+} (Table 1), the binding of a metal ion in the catalytic metal ion site is accompanied by a change in the torsion angle for the side chain of aspartic acid 192 to anywhere between 60° and −120°, as was observed with Zn^{2+}, Cu^{2+}, and Cd^{2+} even at relatively low concentrations (Table 2). Such a change in the torsion angle of aspartic acid 192 results in a much weaker, or no, hydrogen bond with arginine 258 but favorable geometry for binding both the catalytic metal ion and the nucleotide binding metal ion (Figure 5, middle). Although these observations contradict reports that Mn^{2+} binding does not affect the side-chain position of aspartic acid 192 of pol β (Menge et al., 1995), such conclusions may have been based on an erroneous 31-kDa−Mn^{2+} crystal structure[5] or on a 31-kDa−Mn^{2+}−dTTP crystal structure that may not have been refined (Davies et al., 1994). The coordinates for neither structure have been made available for comparisons (Pelletier, 1994).

Despite differences in metal ion coordination geometries and in binding affinities of Mn^{2+} and Mg^{2+}, an overview of the two structures presented in Figure 5 (top) nevertheless suggest that pol β possesses a specific binding site for the part of the nucleotide that is common to all four pol β substrates (dATP, dCTP, dGTP, and dTTP)—the triphosphate and the sugar moieties. There is therefore some crystallographic evidence in support of the idea that, in vivo, initial binding of a nucleotide from solution may be nonselective (that is, non-base-dependent) and occurs primarily via the triphosphate and sugar moieties. An indiscriminate, initial binding step for the sugar−triphosphate moiety that precedes a check against the template for correct base pairing might be an integral part of the mechanism underlying nucleotide selectivity for pol β. Although it could be argued that this type of trial and error mechanism for nucleotide selectivity might be inefficient because the three incorrect nucleotides would be competitive inhibitors of the one correct nucleotide, results from nucleotide soaking experiments in the presence of Mg^{2+} suggest that the initial nucleotide-binding step may be relatively weak and transient, and nucleotides may diffuse in and out of pol β's active site at a rate that is much too fast to affect overall catalysis.

Another significant result from our crystal soaking experiments is that the intimate contacts between the sugar moiety of the nucleotide and the backbone atoms of the thumb subdomain that have now been observed in several pol β structures do not differ significantly from one thumb position to the next, as is evident from comparisons of ddCTP binding in an open versus a closed pol β active site structure (Figure 5, bottom). Since it is not clear from any of the pol β structures determined thus far what, specifically, causes pol β's thumb subdomain to close upon nucleotide binding (Pelletier et al., 1996), it may be that the favorable hydrophobic and van der Waals contacts observed between the thumb and sugar (Figure 5, bottom) are the dominant forces responsible for coupling the movements of the nucleotide with the thumb subdomain. In fact, because structural data suggest that the energy difference between an opened and a closed thumb is relatively small (Pelletier et al., 1996), the thumb subdomain might play a passive role in nucleotide selectivity and may move only in response to nucleotide movement, at least in the initial stages of the thumb closing process.

Although somewhat counterintuitive, the idea of a flexible thumb subdomain moving only in response to nucleotide movement is consistent with proposals that the 8-kDa domain of pol β bends the single-stranded template of a gapped-DNA substrate down into the active site by 90° during processive polymerization (Pelletier et al., 1996). In addition to causing greater sensitivity to DNA mismatches at the active site, yet another useful function of such a bend in the template may be to reduce (or to eliminate) contacts that the template has with an open thumb subdomain and this, in turn, forces any coupled movement between a bent template and an open thumb to rely heavily on the nature of the bound nucleotide, which interacts with both (Pelletier et al., 1996). When pol β structural data (Pelletier et al., 1994, 1996; Sawaya et al., 1994) are combined with pre-steady-state kinetic data from many different polymerases (Kuchta et al., 1987; Patel et al., 1991; Wong et al., 1991; Erie et al., 1993; Spence et al., 1995; Frey et al., 1995; Werneburg et al., 1996), all results point to an induced-fit mechanism for polymerase fidelity whereby, in vivo, only the correct nucleotide can trigger a global, rate-limiting conformational change, in which both a bent DNA template and a flexible thumb subdomain simultaneously close down on the polymerase active site and allow the nucleotidyl transfer reaction to occur.

[5] Our metal ion binding results contradict observations by others (Davies et al., 1994), who report that two bound Mn^{2+} ions are clearly observed in pol β's active site when 31-kDa apoenzyme crystals are soaked in 5 mM $MnCl_2$. Despite efforts to reproduce their conditions, we have not observed this kind of metal ion binding behavior in any pol β crystals, including Mn^{2+}-soaked 31-kDa apoenzyme crystals (Pelletier et al., 1994; Sawaya et al., 1994; Pelletier & Sawaya, 1996a). The only circumstance under which we have produced an electron density map resembling the one reported in their Figure 6A (Davies et al., 1994) was when rat pol β 31-kDa apoenzyme crystals had been soaked in a solution of $K_3UO_2F_5$, a common heavy-atom reagent that had been utilized by those authors in their crystal structure work. Reflection and coordinate files for the Mn^{2+}-soaked 31-kDa crystal structures from this laboratory (Sawaya et al., 1994; Pelletier & Sawaya, 1996a) have the PDB identification codes 1BPC and 1NOM. Neither the reflection file nor the coordinate file for the Mn^{2+}-soaked 31-kDa crystal structure as reported by others (Davies et al., 1994) has been made available. In that it has been proposed that RNase H may have a two-metal-ion-mediated catalytic mechanism that is similar to that of DNA polymerases (Davies et al., 1991, 1994; Steitz & Steitz, 1993), it should be noted that there are analogous disagreements in the literature concerning the active-site metal ion binding behavior of RNase H, where reports that two metal ions bind in the active site of RNase H (Davies et al., 1991) contradict observations by others (Katayanagi et al., 1993; Huang & Cowan, 1994). Neither the reflection file nor the coordinate file for the Mn^{2+}-soaked RNase structure in question (Davies et al., 1991) has been made available.

ACKNOWLEDGMENT

We thank the personnel of the N. H. Xuong Laboratory for aid in data collection, especially C. Nielsen, N. Nguyen, and D. Sullivan. This work was supported in part by grants

from the National Institutes of Health (NIH), the R. A. Welch Foundation, and a grant of computing time from the San Diego Super Computer Center.

REFERENCES

Beard, W. A., Osherhoff, W. P., Prasad, R., Sawaya, M. R., Jagu, M., Wood, T. G., Kraut, J., Kunkel, T. A., & Wilson, S. H. (1996) *J. Biol. Chem. 271*, 12141−12144.

Bebenek, K., Abbotts, J., Wilson, S. H., & Kunkel, T. A. (1993) *J. Biol. Chem. 268*, 10324−10334.

Beckman, R. A., Mildvan, A. S., & Loeb, L. A. (1985) *Biochemistry 24*, 5810−5817.

Beese, L. S., Friedman, J. M., & Steitz, T. A. (1993) *Biochemistry 32*, 14095−14101.

Berg, P., Faucher, H., & Chamberlin, M. (1963) In *Informational Macromolecules* (Vogel, H. J., Bryson, V., & Lampen, J. O., Eds.) pp 467−482, Academic Press, New York.

Bernard, C. (1927) in *An Introduction to the Study of Experimental Medicine* (Green, H. C., Ed.) Macmillan, New York.

Bessman, M. J., Lehman, I. R., Simms, E. S., & Kornberg, A. (1958) *J. Biol. Chem. 233*, 171−177.

Braun, W., Vasak, M., Robbins, A. H., Stout, C. D., Wagner, G., Kagi, J. H., & Wuthrich, K. (1992) *Proc. Natl. Acad. Sci. U.S.A. 89*, 10124−10128.

Burgers, P. M. J., & Eckstein, F. (1979) *J. Biol. Chem. 254*, 6889−6893.

Chang, L. M. S., & Bollum, F. J. (1973) *J. Biol. Chem. 248*, 3398−3404.

Cherian, M. G., Howell, S. B., Imura, N., Klassen, C. D., Koropatnick, J., Lazo, J. S., & Waalkes, M. P. (1994) *Toxicol. Appl. Pharmacol. 126*, 1−5.

Cherrington, J. M., Allen, S. J., McKee, B. H., & Chen, M. S. (1994) *Biochem. Pharmacol. 48*, 1986−1988.

Clark, J. M. (1988) *Nucleic Acids Res. 16*, 9677−9686.

Clark, J. M., Joyce, C. M., & Beardsley, G. P. (1987) *J. Mol. Biol. 198*, 123−127.

Copeland, W. C., Naomi, K. L., & Wang, T. S.-F. (1993) *J. Biol. Chem. 268*, 11041−11049.

da Silva, J. J. R. F., & Williams, R. J. P. (1991) *The Biological Chemistry of the Elements: The Inorganic Chemistry of Life*, Clarendon, Oxford, England.

Davies, J. F., Hostomska, Z., Hostomsky, Z., Jordan, S. R., & Matthews, D. A. (1991) *Science 252*, 88−95.

Davies, J. F., Almassy, R. J., Hostomska, Z., Ferre, R. A., & Hostomsky, Z. (1994) *Cell 76*, 1123−1133.

Demerec, M., & Hanson, J. (1951) *Cold Spring Harbor Symp. Quant. Biol. 16*, 215−228.

Dube, D. K., & Loeb, L. A. (1975) *Biochem. Biophys. Res. Commun. 67*, 1041−1046.

Eckert, K. A., & Kunkel, T. A. (1993a) *J. Biol. Chem. 268*, 13462−13471.

Eckert, K. A., & Kunkel, T. A. (1993b) *Nucleic Acids Res. 21*, 5212−5220.

Eigen, M. (1963) *Pure Appl. Chem. 6*, 97−115.

El-Deiry, W. S., Downey, K. M., & So, A. G. (1984) *Proc. Natl. Acad. Sci. U.S.A. 81*, 7378−7382.

El-Deiry, W. S., So, A. G., & Downey, K. M. (1988) *Biochemistry 27*, 546−553.

Erie, D. A., Hajiseyedjavadki, Q., Young, M. C., & von Hippel, P. H. (1993) *Science 262*, 867−873.

Evans, S. V. (1993) *J. Mol. Graphics 11*, 134−138.

Fersht, A. R., Shi, J.-P., & Tsui, W.-C. (1983) *J. Mol. Biol. 165*, 655−667.

Freese, E. B., & Freese, E. (1967) *Proc. Natl. Acad. Sci. U.S.A. 57*, 650−657.

Frey, M. W., Sowers, L. C., Miller, D. P., & Benkovic, S. J. (1995) *Biochemistry 34*, 9185−9192.

Fry, M., & Loeb, L. A. (1992) *Proc. Natl. Acad. Sci., U.S.A. 89*, 763−767.

Gillin, F. D., & Nossal, N. G. (1976) *J. Biol. Chem. 251*, 5225−5232.

Goodman, M. F., Keener, S., Guidotti, S., & Branscomb, E. W. (1983) *J. Biol. Chem. 258*, 3469−3475.

Hall, Z. W., & Lehman, I. R. (1968) *J. Mol. Biol. 36*, 321−333.

Hamlin, R. (1985) *Methods Enzymol. 114*, 416−452.

Hartwig, A. (1995) *BioMetals 8*, 3−11.

Hibner, U., & Alberts, B. M. (1980) *Nature 205*, 300−305.

Holm, L., & Sander, C. (1995) *Trends Biochem. Sci. 20*, 345−347.

Howard, A. J., Nielsen, C., & Xuong, H. H. (1985) *Methods Enzymol. 114*, 452−472.

Huang, H. W., & Cowan, J. A. (1994) *Eur. J. Biochem. 219*, 253−260.

Katayanagi, K., Okumura, M., & Morikawa, K. (1993) *Proteins: Struct., Funct., Genet. 17*, 337−346.

Kim, S. J., Lewis, M. S., Knutson, J. R., Porter, D. K., Kumar, A., & Wilson, S. H. (1994) *J. Mol. Biol. 244*, 224−235.

Kim, H., Feil, I. K., Verlinde, C. L., Petra, P. H., & Hol, W. G. (1995) *Biochemistry 34*, 14975−14986.

Kohlstaedt, L. A., Wang, J., Friedman, J. M., Rice, P. A., & Steitz, T. A. (1992) *Science 256*, 1783−1790.

Kornberg, A., & Baker, T. A. (1992) *DNA Replication*, 2nd ed., Freeman, San Francisco, CA.

Krauss, S. W., & Linn, S. (1980) *Biochemistry 19*, 220−228.

Kuchta, R. D., Mizrahi, V., Benkovic, P. A., Johnson, K. A., & Benkovic, S. J. (1987) *Biochemistry 26*, 8410−8417.

Kunkel, T. A. (1985) *J. Biol. Chem. 260*, 12866−12874.

Kunkel, T. A. (1992) *J. Biol. Chem. 267*, 18251−18254.

Kunkel, T. A. (1993) *Nature 265*, 207−208.

Kunkel, T. A., & Loeb, L. A. (1979) *J. Biol. Chem. 254*, 5718−5725.

Linn, S., Kairis, M., & Holliday, N. (1976) *Proc. Natl. Acad. Sci. U.S.A. 73*, 2818−2822.

Margerum, D. W., Cayley, G. R., Weatherburn, D. C., & Pagenkopf, G. K. (1978) in *Coordination Chemistry* (Martell, A. E., Ed.) p 1, American Chemical Society, Washington, DC.

Martin, R. B. (1990) in *Metal Ions in Biological Systems* (Sigel, H., & Sigel, A., Eds.) Vol. 26, Chapt. 1, Dekker, New York.

Menge, K. L., Hostomsky, Z., Nodes, B. R., Hudson, G. O., Rahmati, S., Moomaw, E. W., Almassy, R. J., & Hostomska, Z. (1995) *Biochemistry 34*, 15934−15942.

Moews, P. C., & Kretsinger, R. H. (1975) *J. Mol. Biol. 91*, 201−225.

Mosbaugh, D. W., & Meyer, R. R. (1982) *J. Biol. Chem. 255*, 10239−10247.

Mosbaugh, D. W., & Linn, S. (1983) *J. Biol. Chem. 258*, 108−118.

Ollis, D. L., Brick, P., Hamlin, R., Xuong, N. G., & Steitz, T. A. (1985) *Nature 313*, 762−766.

Orgel, A., & Orgel, L. E. (1965) *J. Mol. Biol. 14*, 453−457.

Patel, S. S., Wong, I., & Johnson, K. A. (1991) *Biochemistry 30*, 511−525.

Pedersen, L. C., Benning, M. M., & Holden, H. M. (1995) *Biochemistry 34*, 13305−13311.

Pelletier, H. (1994) *Science 266*, 2025−2026.

Pelletier, H., & Sawaya, M. R. (1996) *Biochemistry 35*, 12778−12787.

Pelletier, H., Sawaya, M. R., Kumar, A., Wilson, S. H., & Kraut, J. (1994) *Science 264*, 1891−1903.

Pelletier, H., Sawaya, M. R., Wolfle, W., Wilson, S. H., & Kraut, J. (1996) *Biochemistry 35*, 12742−12761.

Satoh, M., Cherian, M. G., Imura, N., & Shimizu, H. (1994) *Cancer Res. 54*, 5255−5257.

Sawaya, M. R., Pelletier, H., Kumar, A., Wilson, S. H., & Kraut, J. (1994) *Science 264*, 1930−1935.

Shinazi, R. F. (1993) *Perspect. Drug Discovery Des. 1*, 151.

Seal, G., Shearman, C. W., & Loeb, L. A. (1978) *J. Biol. Chem. 254*, 5229−5237.

Sirover, M. A., & Loeb, L. A. (1976a) *Science 194*, 1434−1436.

Sirover, M. A., & Loeb, L. A. (1976b) *Biochem. Biophys. Res. Commun. 70*, 812−817.

Sirover, M. A., & Loeb, L. A. (1977) *J. Biol. Chem. 252*, 3605−3610.

Sirover, M. A., Dube, D. K., & Loeb, L. A. (1979) *J. Biol. Chem. 254*, 107−111.

Smith, R. M., Martell, A. E., & Chen, Y. (1991) *Pure Appl. Chem. 63*, 1015−1080.

Snow, E. T., & Xu, L. S. (1991) *Biochemistry 30*, 11238−11245.

Snow, E. T., & Xu, L. S., & Kinney, P. L. (1993) *Chem.-Biol. Interact. 88*, 155−173.

Spence, R. A., Kati, W. M., Anderson, K. S., & Johnson, K. A. (1995) *Science 267*, 988−993.

Steitz, T. A., & Steitz, J. A. (1993) *Proc. Natl. Acad. Sci. U.S.A. 90*, 6498−6502.
Stoner, G. D., Shimkin, M. B., Troxell, M. C., Thompson, T. L., & Terry, L. S. (1976) *Cancer Res. 36*, 1744−1747.
Strand, M., Prolla, T. A., Liskay, R. M., & Petes, T. D. (1993) *Nature 365*, 274−276.
Streisinger, G., Okada, Y., Emrich, J., Newton, J., Tsugita, A., Terzaghi, E., & Inouye, M. (1966) *Cold Spring Harbor Symp. Quant. Biol. 31*, 77−84.
Tabor, S., & Richardson, C. C. (1989) *Proc. Natl. Acad. U.S.A. 86*, 4076−4080.
Tabor, S., & Richardson, C. C. (1990) *J. Biol. Chem. 265*, 8322−8328.
Tabor, S., & Richardson, C. C. (1995) *Proc. Natl. Acad. Sci. U.S.A. 92*, 6339−6343.
Trautner, T. A., Swartz, M. N., & Kornberg, A. (1962) *Proc. Natl. Acad. Sci. U.S.A. 48*, 499−503.
Tronrud, D. E., Ten Eyck, L. F., & Matthews, B. W. (1987) *Acta. Crystallogr. A43*, 489−501.
van de Sande, J. H., Loewen, P. C., & Khorana, H. G. (1972) *J. Biol. Chem. 247*, 6140−6148.
Versieck, J., & Cornelis, R. (1989) *Trace Elements in Human Plasma or Serum*, CRC Press, Boca Raton, FL.
Wang, T. S.-F., & Korn, D. (1982) *Biochemistry 21*, 1597−1608.
Wang, T. S.-F., Eichler, D. C., & Korn, D. (1977) *Biochemistry 16*, 4927−4934.
Watson, J. D., & Crick, F. H. C. (1953) *Cold Spring Harbor Symp. Quant. Biol. 18*, 123.
Werneburg, B. G., Ahn, J., Zhong, X., Hondal, R. J., Kraynov, V. S., & Tsai, M.-D. (1996) *Biochemistry 35*, 7041−7050.
Williams, R. J. P. (1989) in *Zinc in Human Biology* (Mills, C. E., Ed.) Chapt. 2, Springer-Verlag, London.
Wong, I., Patel, S. S., & Johnson, K. A. (1991) *Biochemistry 30*, 526−537.
Yarchoan, R., Mitsuya, H., Myers, C. E., & Broder, S. (1989) *N. Engl. J. Med. 321*, 726−738.

BI9529566